creative commons
COMMONS DEED

저작자표시-비영리-변경금지 2.0 대한민국

이용자는 아래의 조건을 따르는 경우에 한하여 자유롭게

- 이 저작물을 복제, 배포, 전송, 전시, 공연 및 방송할 수 있습니다.

다음과 같은 조건을 따라야 합니다:

저작자표시. 귀하는 원저작자를 표시하여야 합니다.

비영리. 귀하는 이 저작물을 영리 목적으로 이용할 수 없습니다.

변경금지. 귀하는 이 저작물을 개작, 변형 또는 가공할 수 없습니다.

- 귀하는, 이 저작물의 재이용이나 배포의 경우, 이 저작물에 적용된 이용허락조건을 명확하게 나타내어야 합니다.
- 저작권자로부터 별도의 허가를 받으면 이러한 조건들은 적용되지 않습니다.

저작권법에 따른 이용자의 권리는 위의 내용에 의하여 영향을 받지 않습니다.

이것은 이용허락규약(Legal Code)을 이해하기 쉽게 요약한 것입니다.

Disclaimer

dCollection

의학박사 학위논문

전립선암 세포주의 DRG2 수치가 PARP 저해제에 대한 반응을 예측한다.

DRG2 levels in prostate cancer cell lines predict response to PARP inhibitor.

울 산 대 학 교 대 학 원
의 학 과
윤지형

DRG2 levels in prostate cancer cell lines predict response to PARP inhibitor.

지 도 교 수 박 성 찬

이 논문을 의학 박사학위 논문으로 제출함.

2024 년 2 월

울 산 대 학 교 대 학 원
의 학 과
윤 지 형

윤지형의 의학박사 학위 논문을 인준함

심사위원 김 성 철 인

심사위원 박 성 찬 인

심사위원 전 상 현 인

심사위원 문 경 현 인

심사위원 박 정 우 인

심사위원 오 철 규 인

울 산 대 학 교 대 학 원

2024 년 2 월

감사의 글

어느덧 박사과정 2년도 끝이 나고 이렇게 학위 논문도 나오게 되었습니다. 모든 일이 언제나 그렇지만 이 논문 작성에도 특별한 분들이 많은 도움을 주셨습니다. 미흡하나마 감사의 글 올립니다.

우선 석사과정 때부터 지도 학생으로 받아 주시고 주제선정 및 연구 과정 전반에 도움을 많이 주신 박성찬 교수님. 전공의 시절부터 학술적인 것 이외에도 제가 나아가야 할 길이나 인생 전반적인 것에서 조언을 아끼지 않으시고 도움을 많이 주시며 모범을 보여주셨습니다. 진심으로 감사드립니다.

논문주제에 대해 깊게 알고 계시고 작성과정에 많은 도움을 주셨고 심사위원장까지 맡아 주신 김성철 교수님께도 마음 깊이 감사드립니다.

심사위원을 맡아 주신 전상현 교수님, 문경현 교수님, 박정우 교수님, 오철규 교수님께도 이 지면을 빌려 한 번 더 감사드립니다.

실험 전반적인 설계와 실제적인 진행을 해주 신 생의학연구소의 이원혁 박사님과 이정민 학생이 없었다면 역시 이 논문은 탄생하지 못했을 것입니다. 매우 감사합니다.

절 낳고 키워 주셨으며 언제나 응원해주시는 두분 부모님께도 감사드리고 피는 섞이지 않았으나 친자식처럼 물심양면으로 도와주시는 장인 장모님께도 감사드립니다.

마지막으로 언제나 곁에서 격려해주는 반려 이영숙과 해맑은 미소로 힘이 되어주는 딸 윤이서, 언제나 사랑하고 고맙습니다.

ABSTRACT IN ENGLISH

Introduction

Developmentally regulated GTP-binding protein 2 (DRG2) is a protein that regulates microtubule dynamics and G2/M arrest during docetaxel treatment. Poly ADP-ribose polymerase (PARP) acts as an important repair system for DNA damage caused by docetaxel treatment. The G2/M arrest is an important process for DNA repair, and therefore there is a close relationship between G2/M arrest and PARP inhibitors. This study investigated whether DRG2 expression affects response to PARP inhibitors (olaparib) using prostate cancer cell lines.

Materials and methods

Prostate cancer cell lines were PC3, DU145, LNCaP-FGC, and LNCaP-LN3. Cell viability was determined using a Cell Counting Kit (CCK) assay; anti-DRG2 antibodies were used for western blotting. Cells were transfected with DRG2 siRNA, and pcDNA6/V5-DRG2 was used to overexpress DRG2. The cell cycle was analyzed using flow cytometry, and apoptosis was detected using the Annexin V cell death assay.

Results

The expression of DRG2 was the highest in LNCaP-LN3, and lowest in DU145 cells. Expressions of p53 in PC3, DU145, and the two LNCaP cell lines were null type, high expression, and wild type, respectively. In PC3 (DRG2 high, p53 null), 10nM docetaxel increased G2/M arrest but no apoptosis was observed; however, subsequent treatment with olaparib promoted apoptosis. In DU145 and LNCaP-FGC (DRG2 low, p53 high expression and wild type), 10nM docetaxel increased sub-G1 but not G2/M arrest and induced apoptosis, whereas olaparib had no additional effect. In LNCaP-LN3 (DRG2 high, p53 wild type), increased sub-G1 and G2/M arrest were observed with 10nM docetaxel.

The 10nM docetaxel induced cell death, and combined 10uM olaparib enhanced cell death. In DRG2 knockdown PC3 (DRG2 low, p53 null), both of docetaxel and olaparib combination treatment had little effect on apoptosis. In DRG2 overexpression DU145 (DRG2 high, p53 high expression), cell death was increased by docetaxel and olaparib combination.

Conclusion

DRG2 and p53 expreesions play an important role in prostate cancer cell lines treated with docetaxel, and DRG2 levels can predict the response to PARP inhibitors.

GLOSSARY

DRG2: developmentally regulated GTP-binding protein 2

HSPC: hormone sensitive prostate cancer

CRPC: castration-resistant prostate cancer

PARP: poly ADP-ribose polymerase

BRCA: breast cancer susceptibility gene

CCK: Cell Counting Kit

RIPA: radioimmunoprecipitation assay

BSA: bovine serum albumin

TBST: tris-buffered saline with tween®20

siRNAs: small interfering RNAs

siDRG2: siRNAs targeting human DRG2

scRNA: control siRNA

FITC: fluorescein isothiocyanate

PCR: polymerase chain reaction

NHEJ: non-homologous end joining

LIST OF FIGURES

in the cell cycle of PC3 and DU145 cells after treatment with docetaxel and olaparib for 72 h. (**e**) Flow cytometric analysis of PC3 and DU145 cells after treatment with docetaxel and olaparib for 72 h. Cells were stained with Annexin V fluorescein and propidium iodide. (**f**) Viability assay of PC3 cells after treatment with APR-246, docetaxel, and olaparib for 72 h. (**g**) Viability of DU145 cells transfected with scRNA or sip53 after treatment with docetaxel and olaparib for 72 h. (**h**) Viability of PC3 cells transfected with scRNA or siDRG2 after treatment with docetaxel and olaparib for 72 h. (**i**) Viability of DU145-pcDNA6-V5 and DU145-DRG2/pcDNA6-V5 cells treated with docetaxel and olaparib for 72 h. Cell viability was determined using the CCK assay.

Figure 5. Changes in prostate cancer cell lines (PC3, DU145) caused by administration of etoposide and PARP inhibitor. (**a**) Cell Viability of PC3 and DU145 cells after treatment with etoposide and olaparib for 72 h. (**b**) Flow cytometry analysis showing differences in the cell cycle of PC3 and DU145 cells after treatment with etoposide and olaparib for 72 h.

Table of contents

INTRODUCTION

Prostate cancer has the highest incidence rate among cancer malignancies, accounting for 29% of cancers in men in the United States in 2023 [1]. The incidence of prostate cancer has also increased in Korea due to westernized eating habits and an increase in average life expectancy [2]. There are two types of prostate cancer: hormone sensitive prostate cancer (HSPC) and castration-resistant prostate cancer (CRPC), which is hormone-refractory. HSPC can be treated by suppressing associated hormones, whereas CRPC is treated with chemotherapy such as docetaxel [3]. Docetaxel was approved by the FDA as the first-line treatment for CRPC in 2004 [4]. However, the average survival period of patients treated with docetaxel is 59.1 months, and the 5-year survival rate is as low as 49% [5]. Therefore, identifying the underlying mechanisms to overcome docetaxel resistance and increase its efficacy in the treatment of prostate cancer is crucial.

Recently, new drug classes have been approved for CRPC treatment, one of which is Poly ADP-ribose polymerase (PARP) inhibitors [4]. However, many patients who received PARP inhibitor treatment have acquired resistance [6]. In addition, the use of PARP inhibitors is limited by the fact that they are effective against breast cancer susceptibility gene (BRCA) mutations, which exist in only about 20% of prostate cancer patients. These PARP inhibitors are effective in cells, which have undergone G2/M phase arrest [4]. Moreover, we previously confirmed that cells undergo G2/M arrest due to the expression of developmentally regulated GTP-binding protein 2 (DRG2), caused by docetaxel treatment [7]. As G2/M arrest was observed after docetaxel treatment in cells expressing DRG2, we hypothesized that treatment with a PARP inhibitor would be effective.

This study aimed to determine the effect of DRG2 expression on the effectiveness of PARP inhibitors. We hypothesized that G2/M arrest caused by DRG2 expression results in cell death via PARP inhibitors.

METERIALS AND METHODS

Drugs

Docetaxel (Sanofi-Aventis U.S. LLC, Bridgewater, NJ, USA), olaparib (Selleck Chemicals, Houston, TX, USA), and etoposide (Boryung Pharmaceutical Co., Ltd., Seoul, Republic of Korea) were used at the indicated concentrations.

Cell culture

The prostate cancer cell lines PC3, DU145, LNCaP-FGC, and LNCaP-LN3 were obtained from the Korean Cell Line Bank (Seoul, Republic of Korea). All cell lines were cultured in RPMI-1640 medium (WELGENE, Gyeongsan, Republic of Korea) supplemented with 10% fetal bovine serum (Invitrogen, Carlsbad, CA, USA) and 1% penicillin/streptomycin (Invitrogen), at 37 °C in a humidified chamber containing 5% CO_2.

Cell viability assay

Cell viability was analyzed at the indicated times using a D-Plus™ CCK cell viability assay kit (Dongin Biotech, Seoul, Republic of Korea) according to the manufacturer's instructions. Absorbance was measured at 450 nm (OD450) for each well using a Wallac Vector 1420 Multilabel Counter (EG&G Wallac, Turku, Finland).

Western blot analysis and siRNA transfection

Total protein was extracted using radioimmunoprecipitation assay (RIPA) buffer containing protease and phosphatase inhibitors (Thermo Fisher Scientific, Waltham, MA, USA), and the protein concentration was determined using a Bradford protein assay kit (Bio-Rad Laboratories, Hercules, CA, USA). Proteins were separated via electrophoresis on an 8–12% SDS-polyacrylamide gel and transferred onto a nitrocellulose membrane (Amersham International, Little Chalfont, UK). Membranes were blocked with 5% bovine serum albumin (BSA; bioWORLD, Dublin, OH, USA) in

tris-buffered saline with tween®20 (TBST) for 1 h at room temperature. Membranes were subsequently washed with TBST and incubated overnight at 4 °C with the following primary antibodies: DRG2 (14743-1-AP; Proteintech, Rosemont, IL, USA), caspase-3 (#9662; Cell Signaling Technology [CST], Danvers, MA, USA), p53 (#2524; CST), cdc2 (#9116; CST), PARP (#9542; CST), Rad 51 (sc-377467; Santa Cruz Biotechnology, Santa Cruz, CA, USA), and β-actin (sc-47778; Sigma-Aldrich Inc., MO, USA) diluted in 5% BSA/TBST. The membranes were again washed with TBST and then incubated for 1 h in a 2,000-fold diluted TBST containing the secondary antibody anti-mouse or anti-rabbit IgG HRP conjugate (Bethyl Laboratories, Montgomery, TX, USA). After washing with TBST, the specific binding of antibodies was detected using an excellent chemiluminescent substrate (ECL) kit (Thermo Fisher Scientific) following the manufacturer's instructions. Small interfering RNAs (siRNAs) targeting human DRG2 (siDRG2; sc-93839), human p53 (sip53; sc-29435), and control siRNA (scRNA; sc-37007) were purchased from Santa Cruz Biotechnology. AMC-HN3 cells (1.5 or 3×10^5) were transfected with each siRNA using Lipofectamine™ RNAiMAX (Invitrogen).

Flow cytometry

Cells were harvested via trypsinization, washed in ice-cold phosphate buffered saline (PBS), fixed in ice-cold 70% ethanol in PBS, centrifuged at 4 °C, and resuspended in chilled PBS. Bovine pancreatic RNAase (Sigma-Aldrich Inc., MO, USA) was added to the fixed cells at a final concentration of 2 μg/mL and the cells were incubated at 37 °C for 30 min. Then, 20 μg/mL of propidium iodide (Sigma-Aldrich) was added to the cells in each group and incubated for 20 min at room temperature. The cells were analyzed by flow cytometry (FACSCalibur; BD Biosciences, San Jose, CA, USA).

Immunofluorescence microscopy

The cells were plated on 18-mm coverslips and fixed with 3.7% paraformaldehyde, permeabilized in 0.1% Triton X-100 in PBS, and blocked in PBS/5% BSA. DRG2 was detected using a DRG2

polyclonal antibody (14743-1-AP; Proteintech) incubated overnight at 4 °C, followed by incubation with fluorescent-conjugated secondary antibodies (Molecular Probes, Eugene, OR, USA). After washing, cells were mounted on glass slides and examined under a DP40 microscope (Olympus, Tokyo, Japan).

Determination of apoptosis by Annexin V/propidium iodide (PI) analysis

Human PC3 cells were seeded on a 60-mm dish and incubated with docetaxel (10 nM) and olaparib (10 μM) for 72 h, washed twice with ice-cold PBS (pH 7.0), and then resuspended in binding buffer (500 μL). Subsequently, fluorescein isothiocyanate (FITC)-Annexin V (5 μL) was added to PI (5 μL) and incubated for 15 min at room temperature in the dark. Samples were analyzed using a fluorescence-activated flow cytometer (NovoCyte Quanteon; Agilent, Santa Clara, CA, USA).

Statistical Analysis

All statistical analyses and calculations were performed using Microsoft Excel spreadsheets and GraphPad Prism version 10 (GraphPad Software, San Diego, CA, USA). Group differences were determined using the Student's t-test or Mann–Whitney U test. Data are expressed as the mean ± standard deviation. All statistical tests were two-sided, and $P < 0.05$ was considered statistically significant.

RESULTS

Characteristics of prostate cancer cell lines

The expressions of DRG2 and p53 were confirmed in prostate cancer cell lines using western blotting. PC3 cells showed null-type DRG2 and p53 expressions, whereas DU145, LNCaP-FGC, and LNCaP-LN3 cells showed confirmed expressions of both DRG2 and p53. Further, p53 expression was higher in DU145 cells than in other cell lines (Fig. 1a).

Expression levels of DRG2 in the prostate cancer cell lines were confirmed using real-time polymerase chain reaction (PCR.) We observed that DRG2 expression was high in PC3 and LNCaP-LN3 cells but low in DU145 and LNCaP-FGC cells (Fig. 1b).

All studied prostate cancer cell lines were treated with docetaxel (0–10 μM) and cell viability was determined after 72 h. The IC50 values were 13.91, 9.04, 7.97, and 5.97 nM in PC3, DU145, LNCaP-FGC, and LNCaP-LN3 cells, respectively. Based on these results, the docetaxel treatment concentration was set at 10 nM for subsequent experiments (Fig. 1c).

Among the prostate cancer cell lines, the CRPC cell lines PC3 and DU145 were used to check cell viability at different time points during docetaxel (10 nM) treatment. PC3 cells showed high DRG2 expression but no p53 expression, whereas DU145 cells showed low DRG2 expression and high p53 expression. Further, cell viability continued to decrease in DU145 cells but became constant in PC3 cells after a certain level. To confirm changes during the recovery period, cell viability was assessed at each period after docetaxel (10 nM) treatment and media changes after 72 h. During the recovery period, cell viability continued to decrease in DU145 cells but recovered in PC3 cells (Fig. 1d).

Figure 1a DRG2 and p53 expressions in prostate cancer cell lines as determined via western blot analysis.

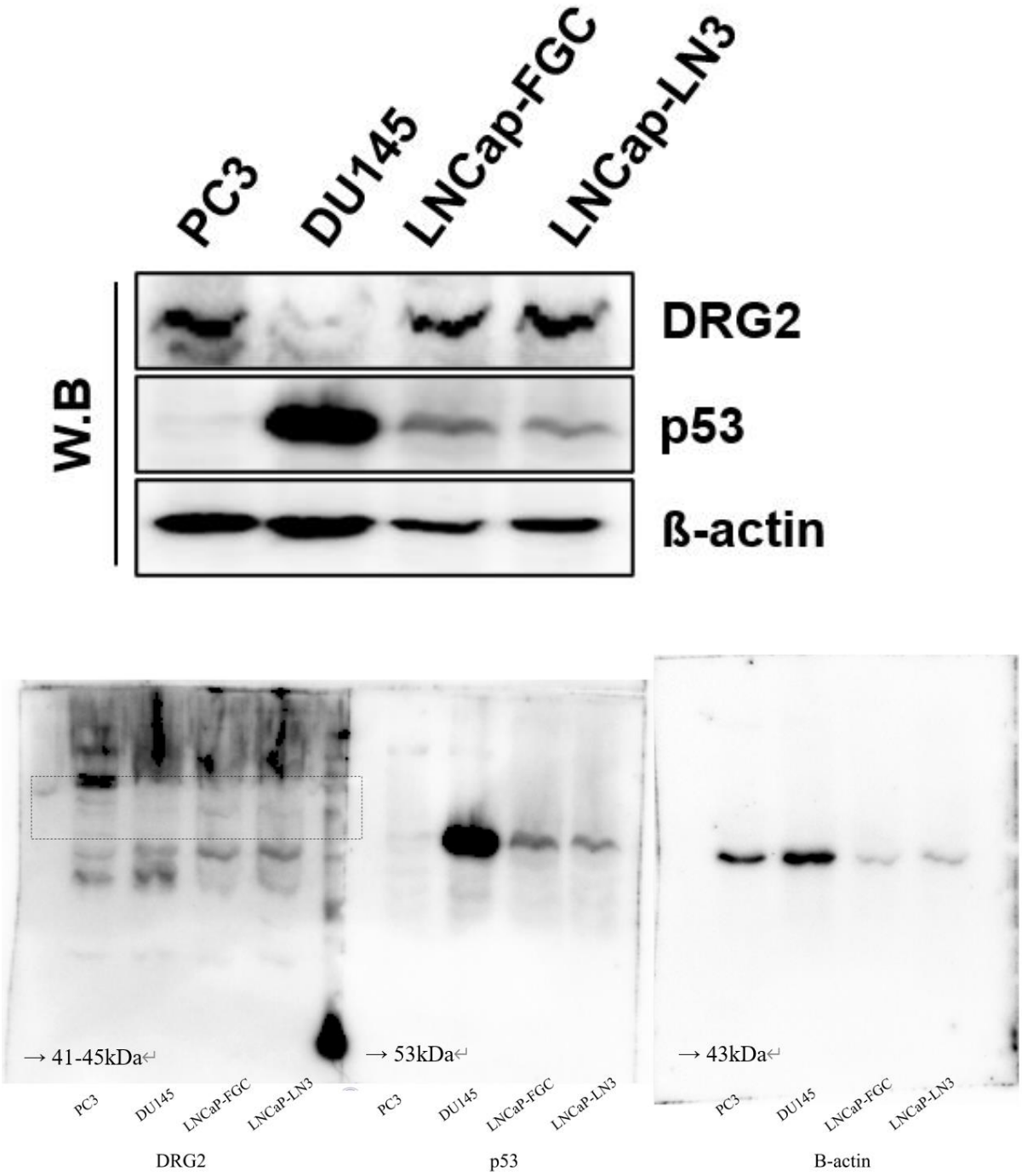

Figure 1b DRG2 expression in prostate cancer cell lines as determined using real-time PCR.

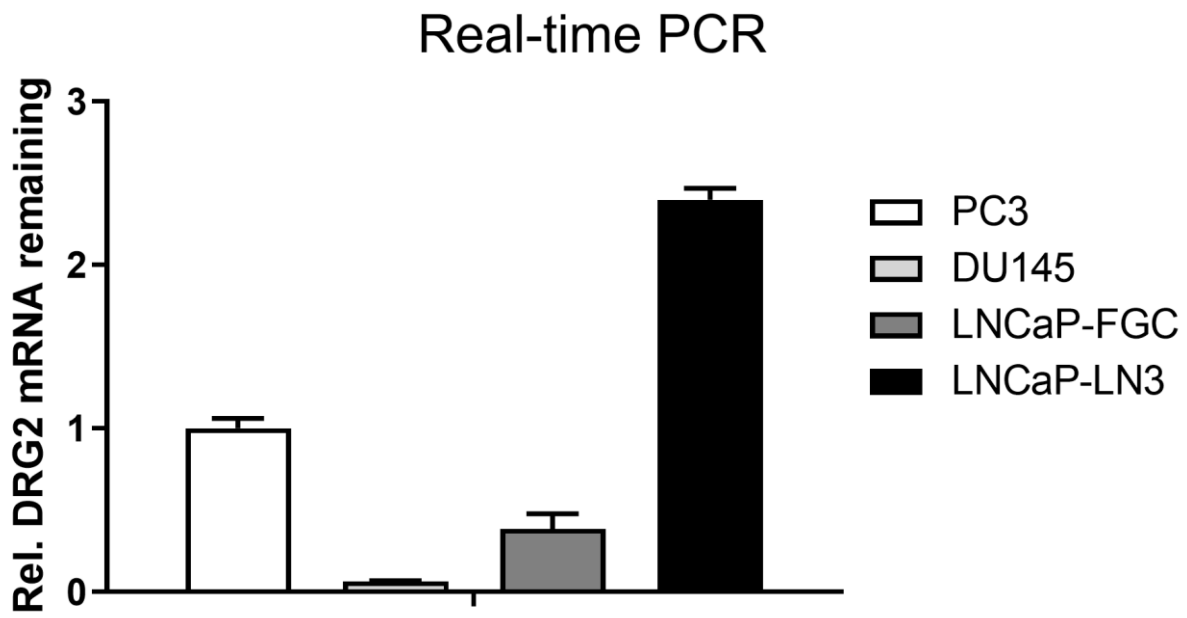

Figure 1c IC50 values of docetaxel on prostate cancer cells were determined using a CCK assay. Cells were exposed to 0–10 μM docetaxel for 72 h.

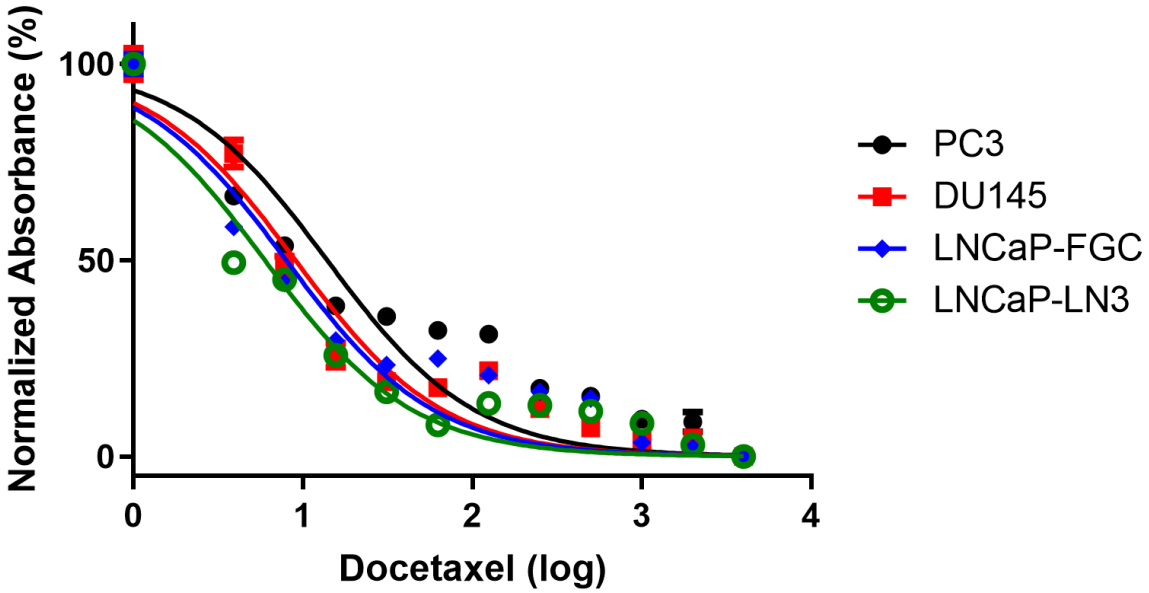

	PC3	DU145	LNCaP-FGC	LNCaP-LN3
IC50 (nM)	13.910	9.042	7.973	5.968

Figure 1d Cell viability of the prostate cancer cell lines after docetaxel treatment for 72 h, determined using a CCK assay.

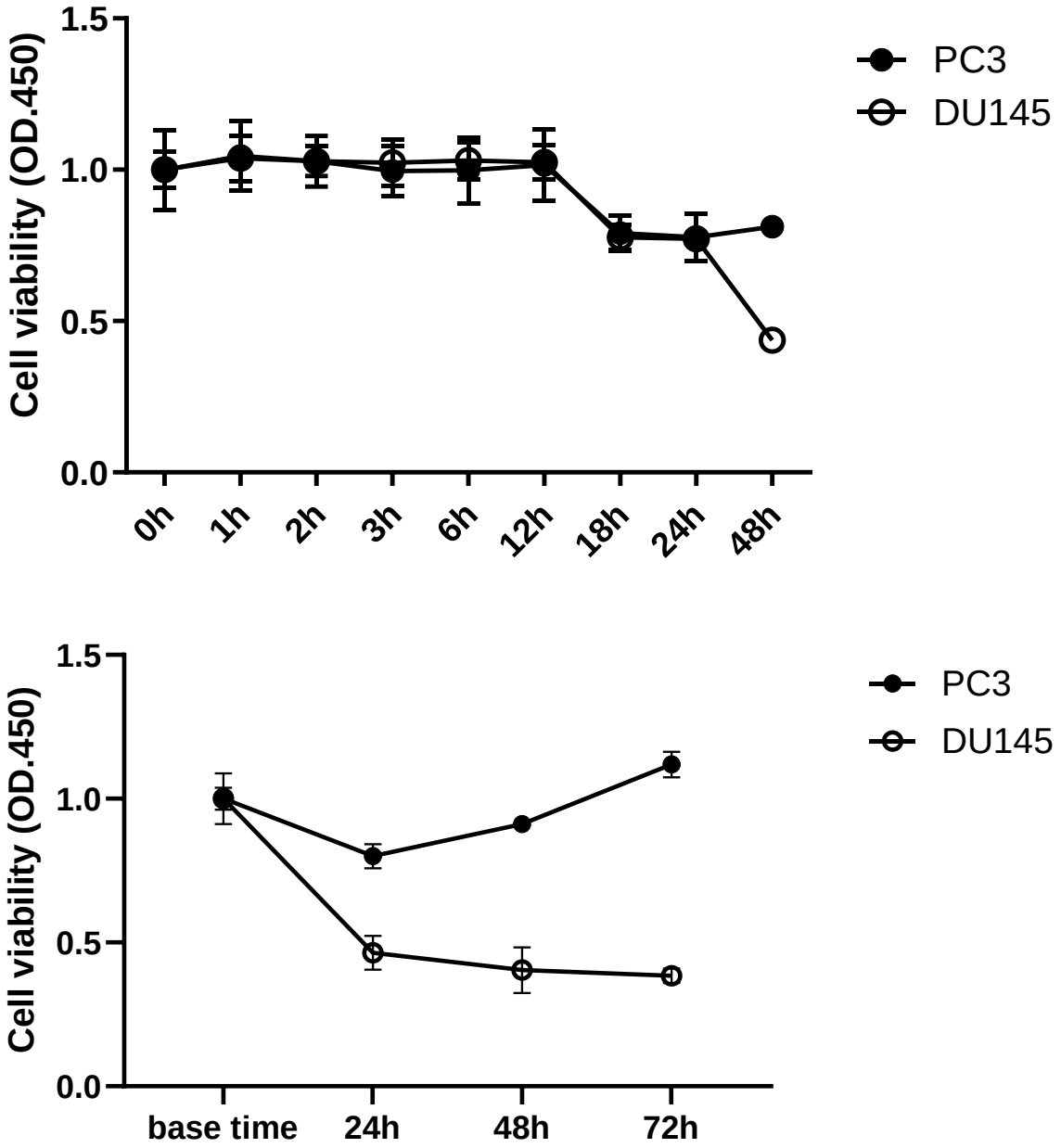

Cell cycle arrest after docetaxel treatment

The prostate cancer cell lines were treated with docetaxel at each concentration, and changes in cell cycle were analyzed using a microscope. As the concentration of docetaxel increased, the number of PC3 cells also increased without showing any decreasing trends. Although the number of LNCaP-LN3 cells decreased, the number of remaining cells increased. The number of LNCaP-FGC and DU145 cells also decreased, but it was confirmed that the cells did not grow (Fig. 2a).

The cell cycle phase of each cell type according to the docetaxel concentration was determined through flow cytometry. In PC3 cells, G2/M arrest increased without a sub-G1 increase; in LNCaP-LN3 cells, both sub-G1 and G2/M increased. In DU145 and LNCaP-FGC cells, only sub-G1 arrest increased, without an increase in G2/M (Fig. 2b).

The expression of proteins related to the cell cycle was determined for each cell line via western blotting after docetaxel administration. In PC3 and LNCaP-LN3 cells, cdc2 expression was observed to decrease (Fig. 2c).

Figure 2a Prostate cancer cell lines were monitored using a microscope after docetaxel treatment.

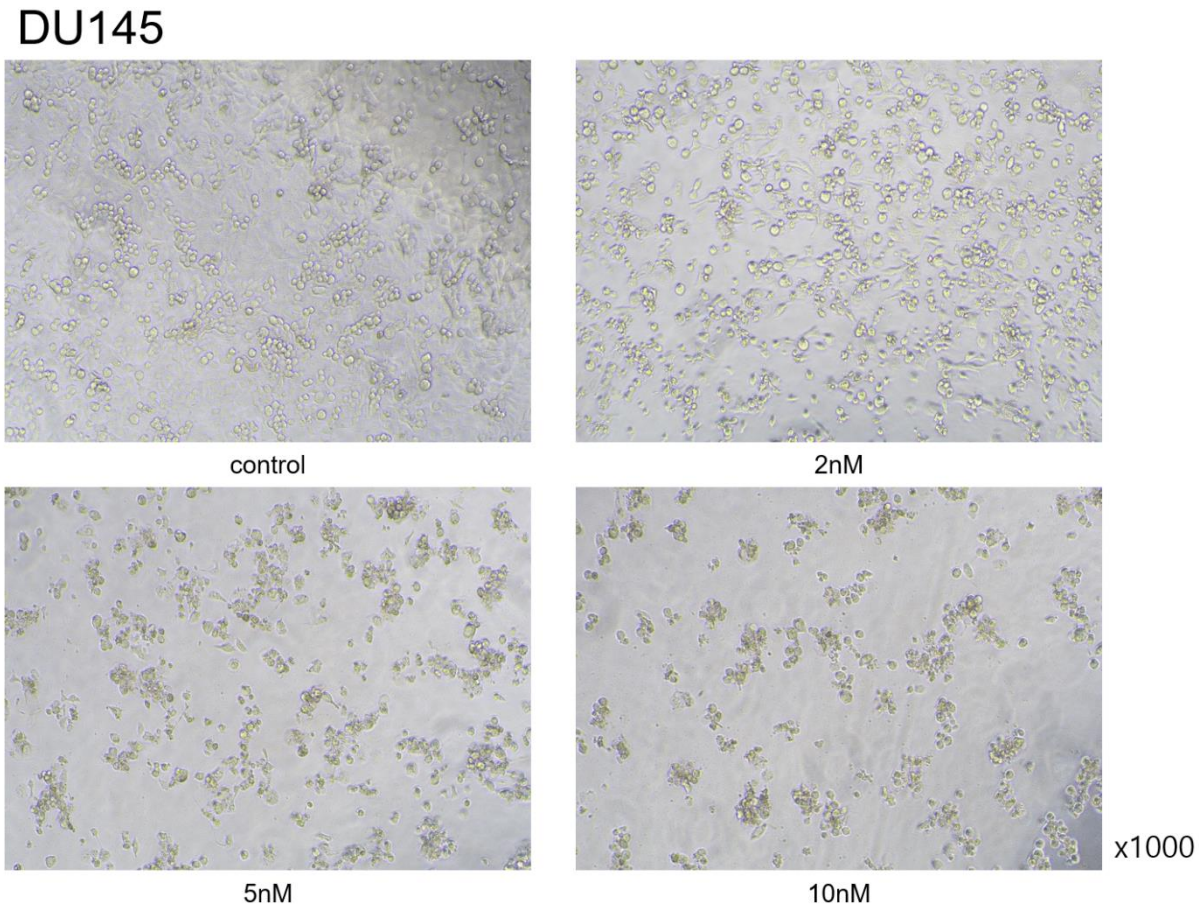

LNCap-FGC

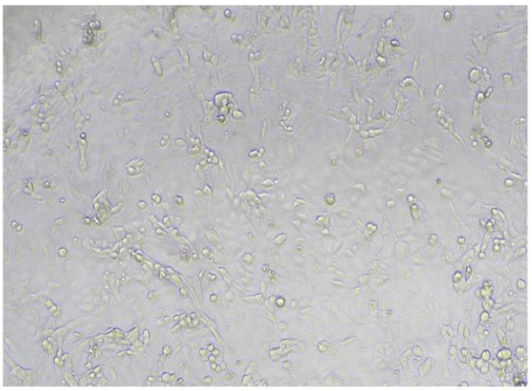

control

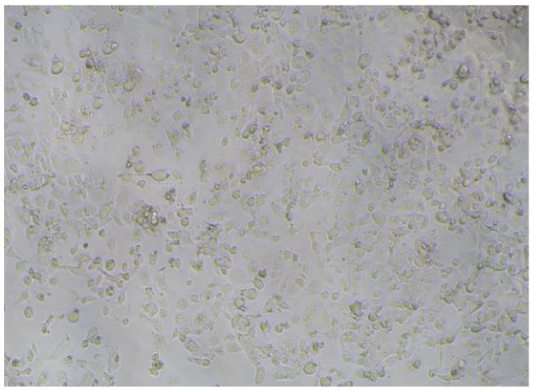

2nM

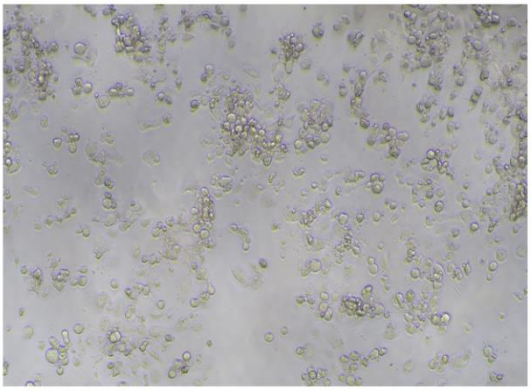

5nM

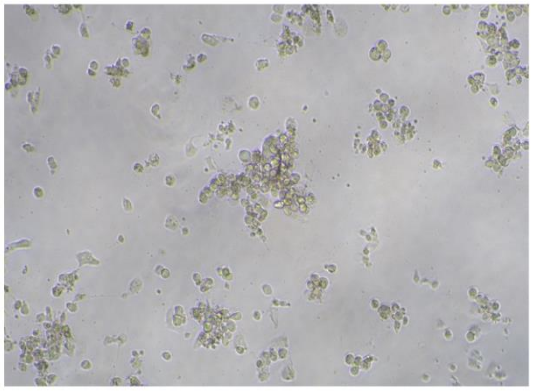

10nM

x1000

LNCap-LN3

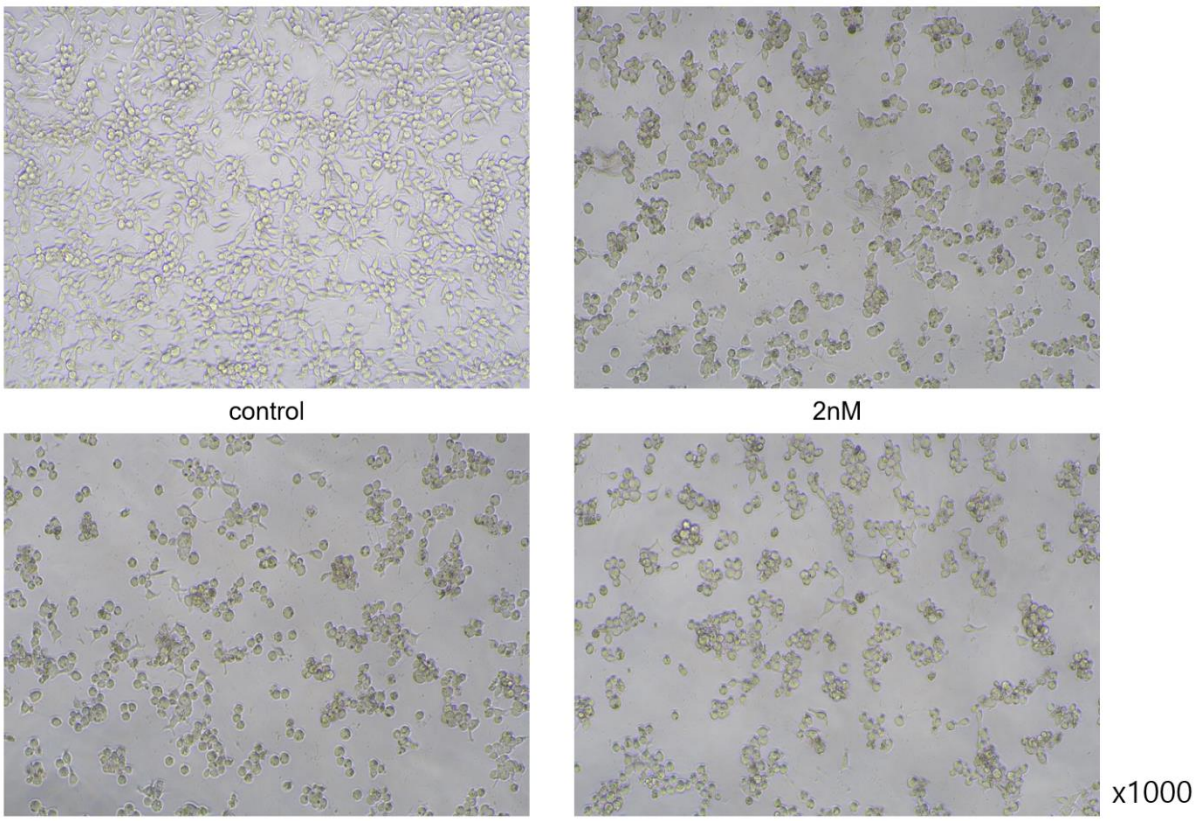

PC3

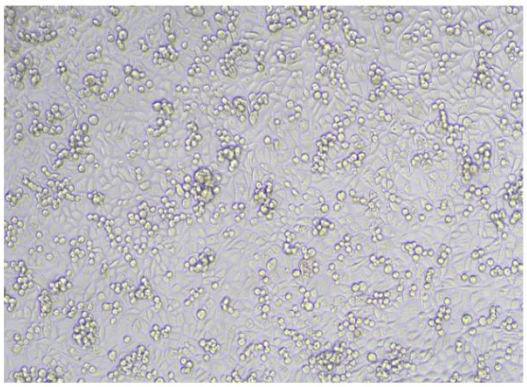

control

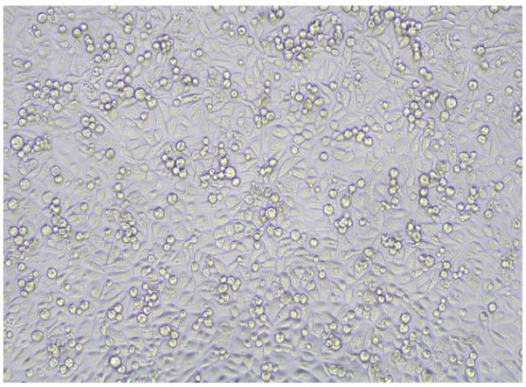

2nM

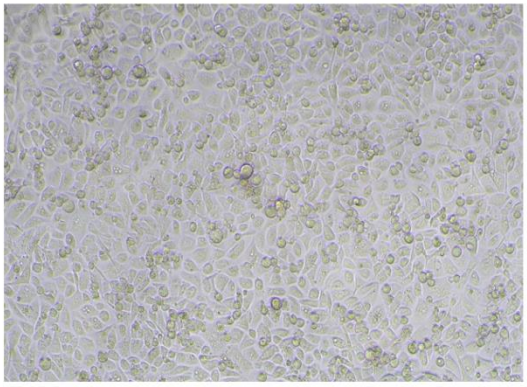

5nM

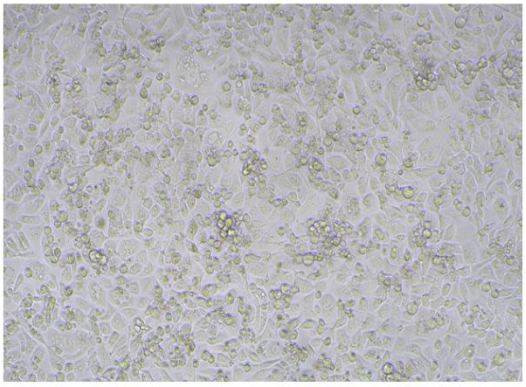

10nM

x1000

Figure 2b Flow cytometry analysis of the docetaxel-treated prostate cancer cells after 72 h.

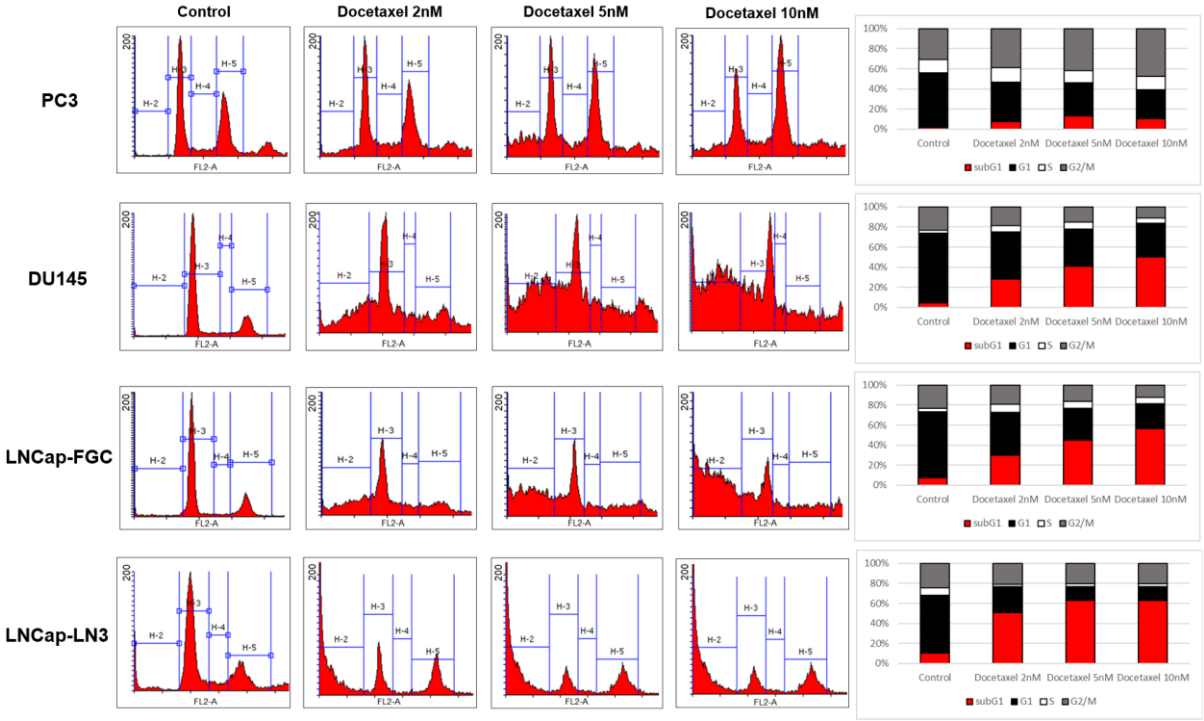

Figure 2c Change in cdc2 expression after docetaxel treatment analyzed via western blot analysis. The graph represents the quality density value as obtained on ImageJ software with β-actin as a control.

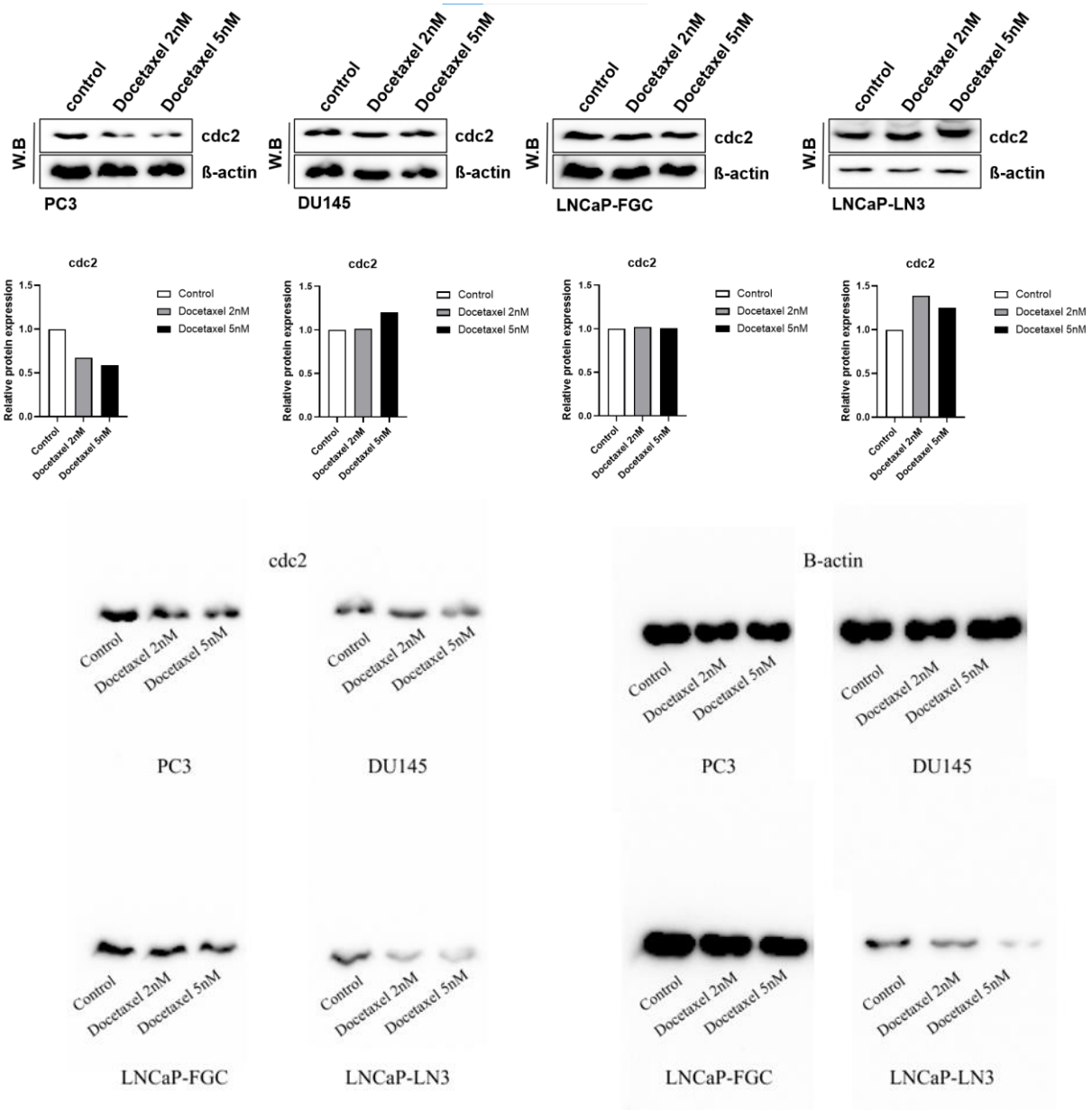

Changes in cell viability based on differences in DRG2 and p53 expressions after docetaxel treatment

PC3 cells with p53 null type expression were treated with 15 μM of APR-246, a p53 activator, followed by docetaxel (10 nM), and cell viability was evaluated. In PC3 cells not treated with APR-246, cell viability did not decrease significantly when treated with docetaxel; however, in PC3 cells treated with APR-246, cell viability decreased (Fig. 3a).

Following p53 knockdown in DU145 cells with low DRG2 expression, cell viability was evaluated after treatment with docetaxel (10 nM). Cell viability decreased with scRNA treatment, but no significant changes were observed in sip53 DU145 (Fig. 3b).

Cytoplasmic and nuclear extractions were performed in PC3 and DU145 cells. After treatment with docetaxel (10 nM), changes in DRG2 in the cytoplasm and nucleus were confirmed through western blotting. After treating PC3 cells with docetaxel, the amount of DRG2 was increased in the nucleus. In DU145 cells, no change in DRG2 expression in the cytoplasm or the nucleus was observed (Fig. 3c).

After treating PC3 cells with docetaxel (10 nM), positional changes in DRG2 were evaluated using immunofluorescence microscopy. Compared with the control, DRG2, which was distributed throughout the cell, migrated to the nucleus in PC3 cells treated with docetaxel (10 nM) (Fig. 3d).

After DRG2 overexpression in DU145 cells, which showed low DRG2 expression, cell viability was evaluated following treatment with docetaxel (10 nM). In DU145-pcDNA6-V5, cell viability was significantly reduced, but in DU145-DRG2/pcDNA6-V5, cell viability was not significantly reduced compared to DU145-pcDNA6-V5 (Fig. 3e).

Flow cytometry confirmed that sub-G1 was increased when DU145-pcDNA6-V5 was treated with 5 nM docetaxel. However, when DU145-DRG2/pcDNA6-V5 cells were treated with docetaxel, the G2/M arrest significantly increased (Fig. 3f).

PC3 cells, which highly express DRG2, were knocked down for DRG2, and cell viability was

evaluated following treatment with docetaxel (10 nM). Cell viability decreased when DRG2-knockdown PC3 cells were treated with docetaxel, but it did not decrease when PC3 cells were treated with docetaxel (Fig. 3g).

Using flow cytometry, DRG2 was knocked down in PC3 cells, where DRG2 expression was high, and the cell cycle was confirmed according to the docetaxel concentration. PC3 cells in the G2/M arrest increased without an increase in the sub-G1, and a sub-G1 increase was confirmed in DRG2-knocked PC3 cells (Fig. 3h).

Figure 3a Cell viability assay in PC3 cells treated with APR-246 and docetaxel for 72 h.

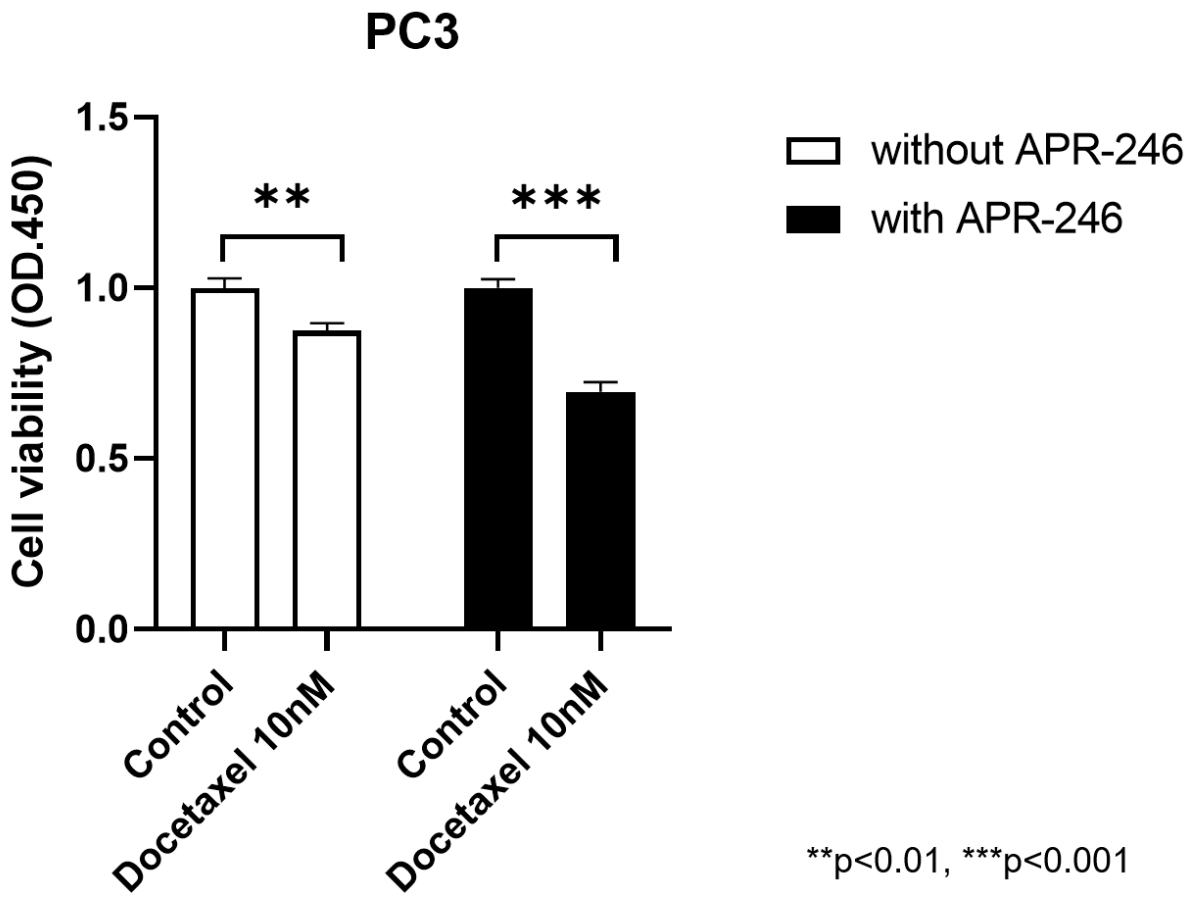

Figure 3b Cell viability assay in DU145 cells transfected with scRNA or sip53 after docetaxel treatment for 72 h.

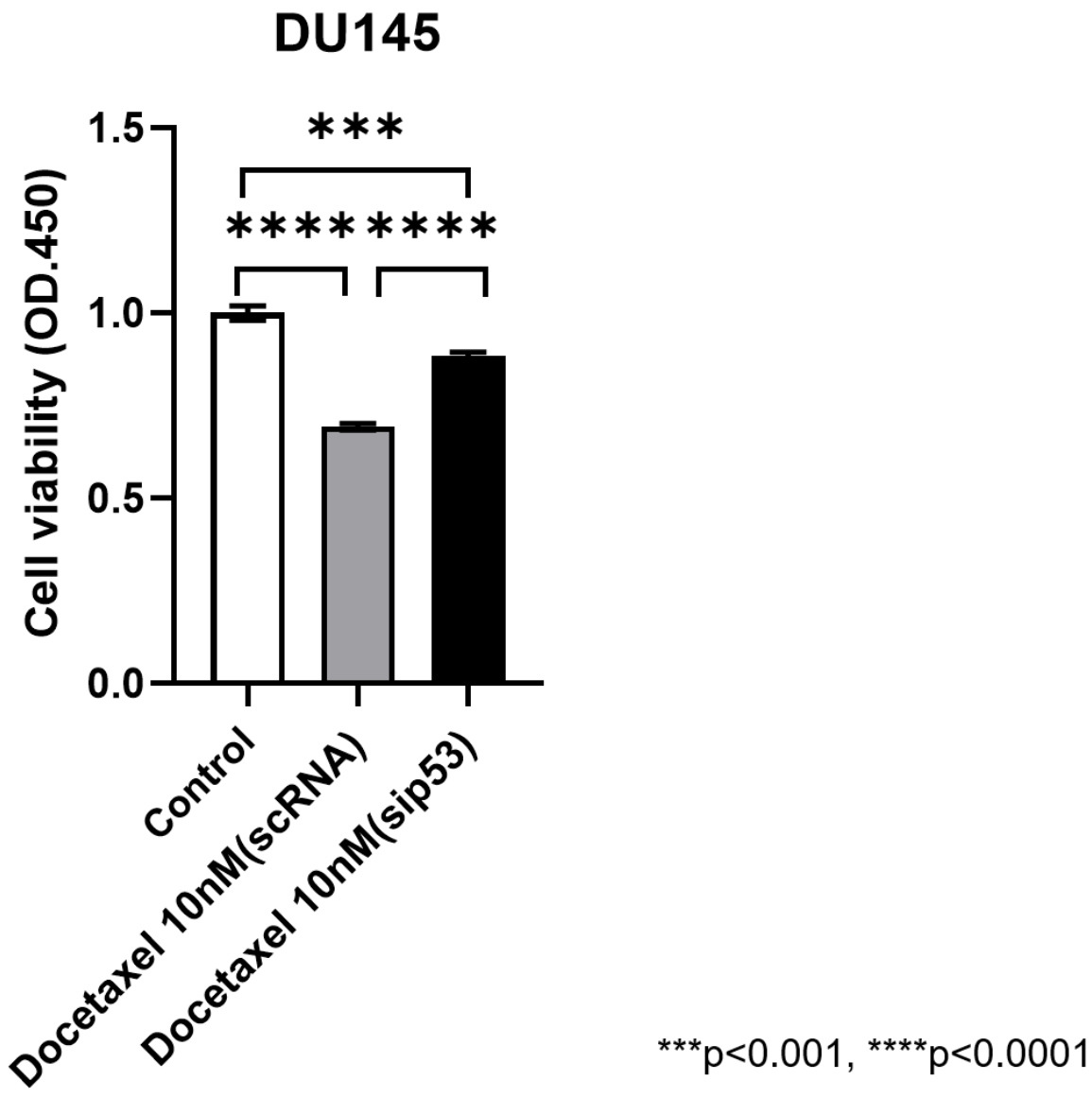

Figure 3c Changes in DRG2 expression in the cytoplasm and nuclear extracts after docetaxel treatment analyzed via western blot analysis.

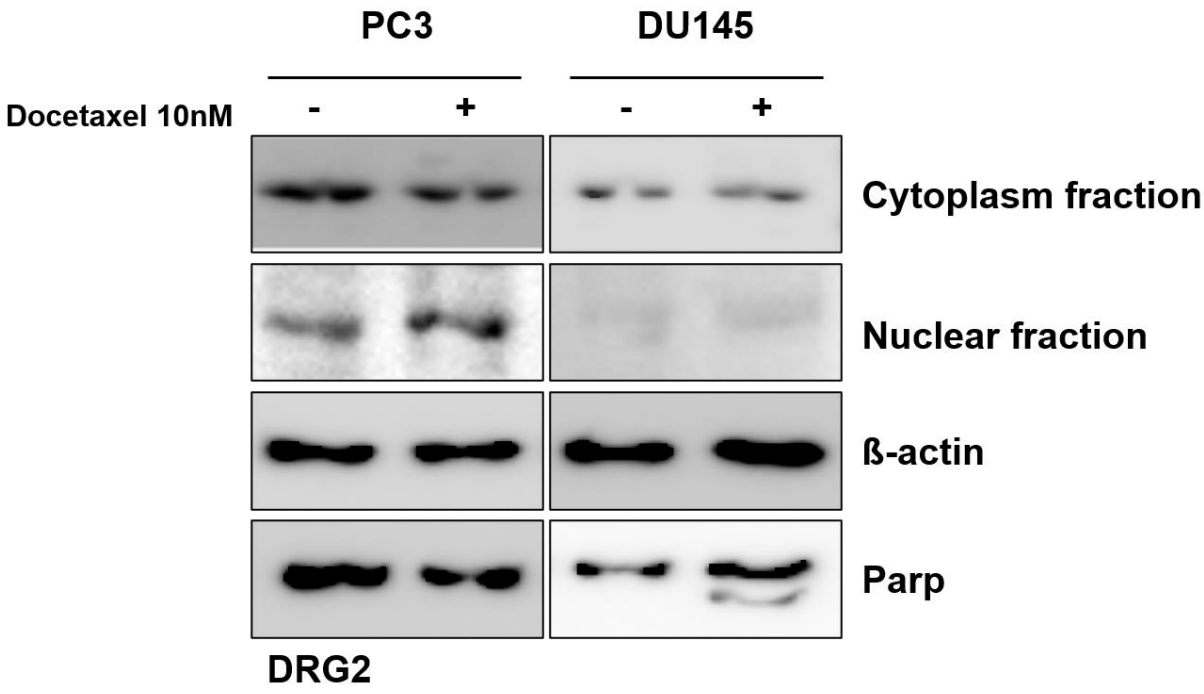

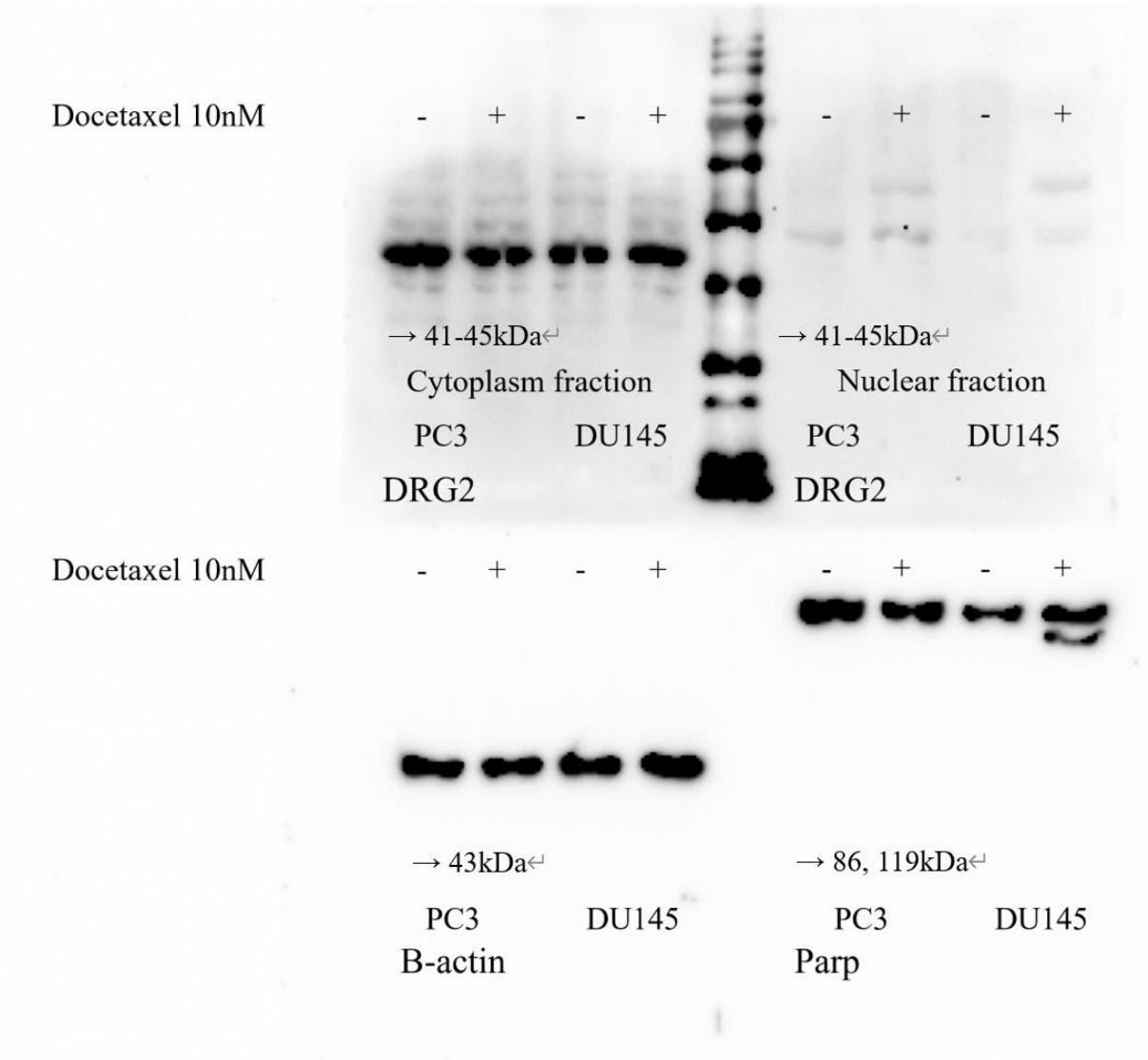
Docetaxel 10nM
- + - + - + - +
→ 41-45kDa
Cytoplasm fraction
PC3 DU145
DRG2
→ 41-45kDa
Nuclear fraction
PC3 DU145
DRG2
Docetaxel 10nM
- + - + - + - +
→ 43kDa
PC3 DU145
B-actin
→ 86, 119kDa
PC3 DU145
Parp

Figure 3d Immunofluorescence microscopy images of PC3 cells after docetaxel treatment.

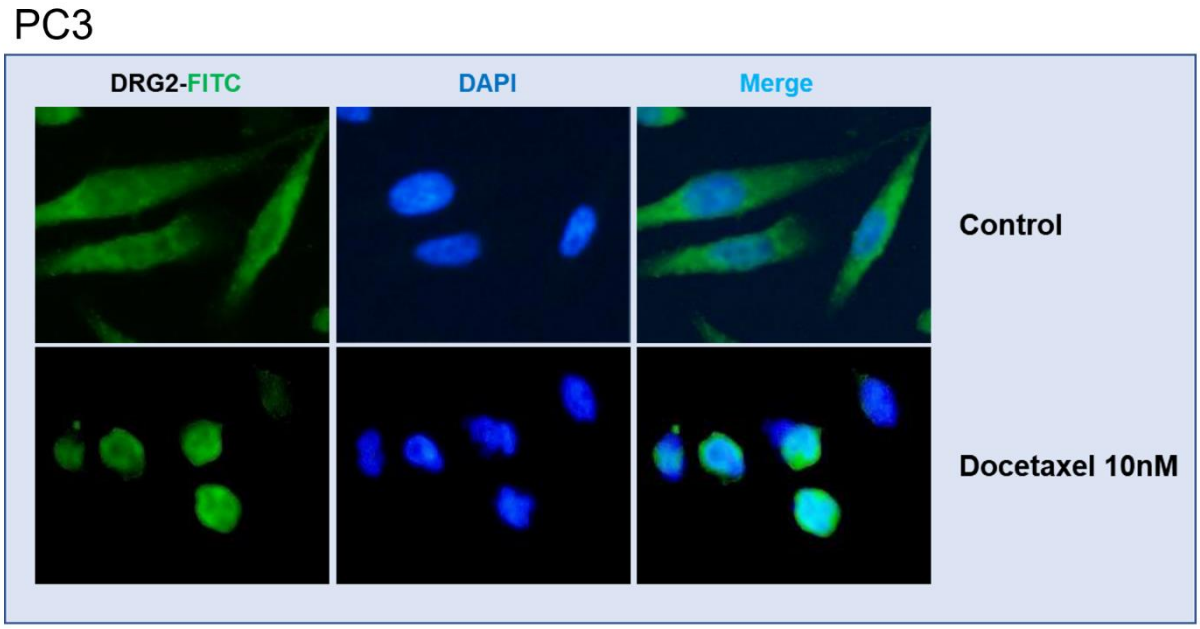

Figure 3e Cell viability assay in DU145-pcDNA6-V5 and DU145-DRG2/pcDNA6-V5 cells after docetaxel treatment for 72 h.

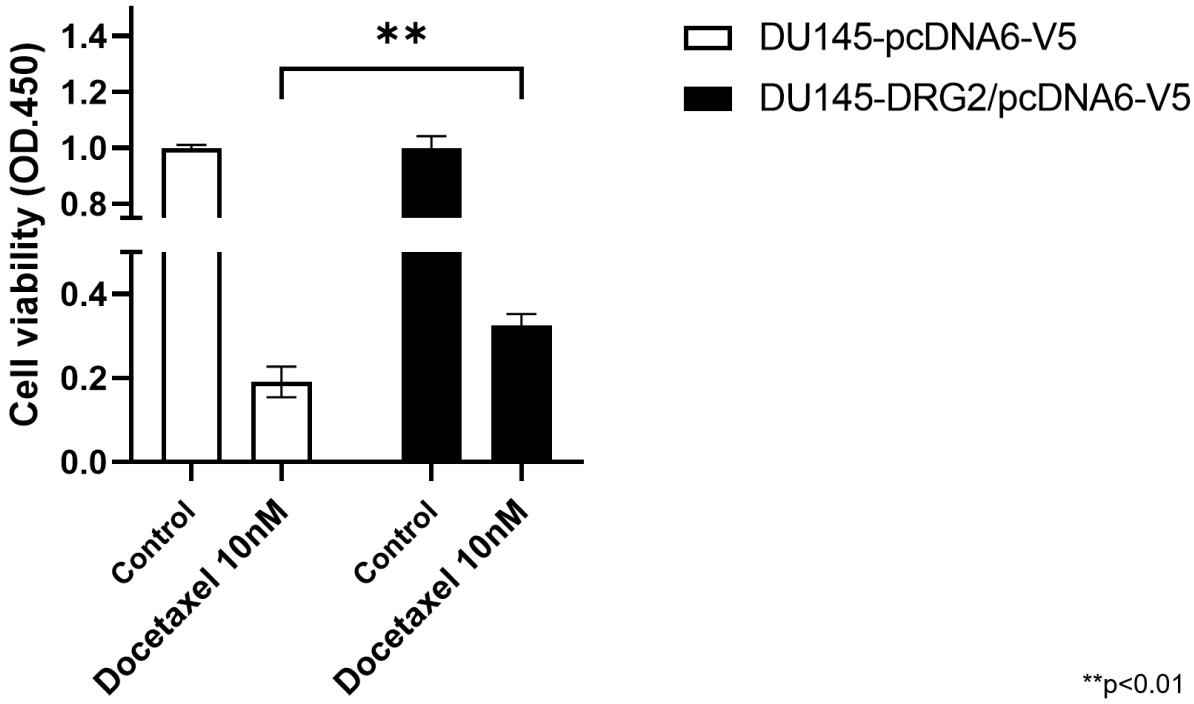

Figure 3f Flow cytometry analysis showing the difference in cell cycles of DU145-pcDNA6-V5 and DU145-DRG2/pcDNA6-V5 cells after treatment with docetaxel for 72 h.

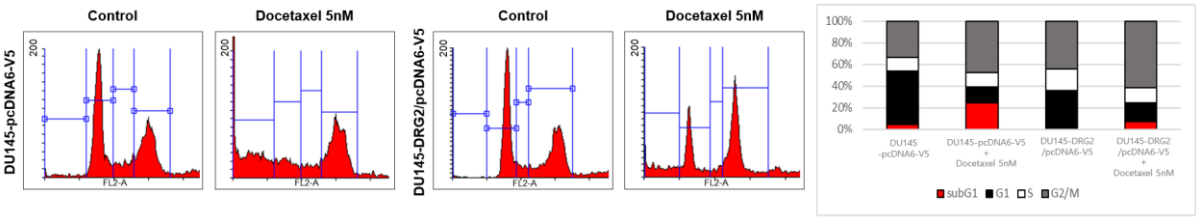

Figure 3g Cell viability assay in PC3 cells transfected with scRNA or siDRG2 after docetaxel treatment for 72 h.

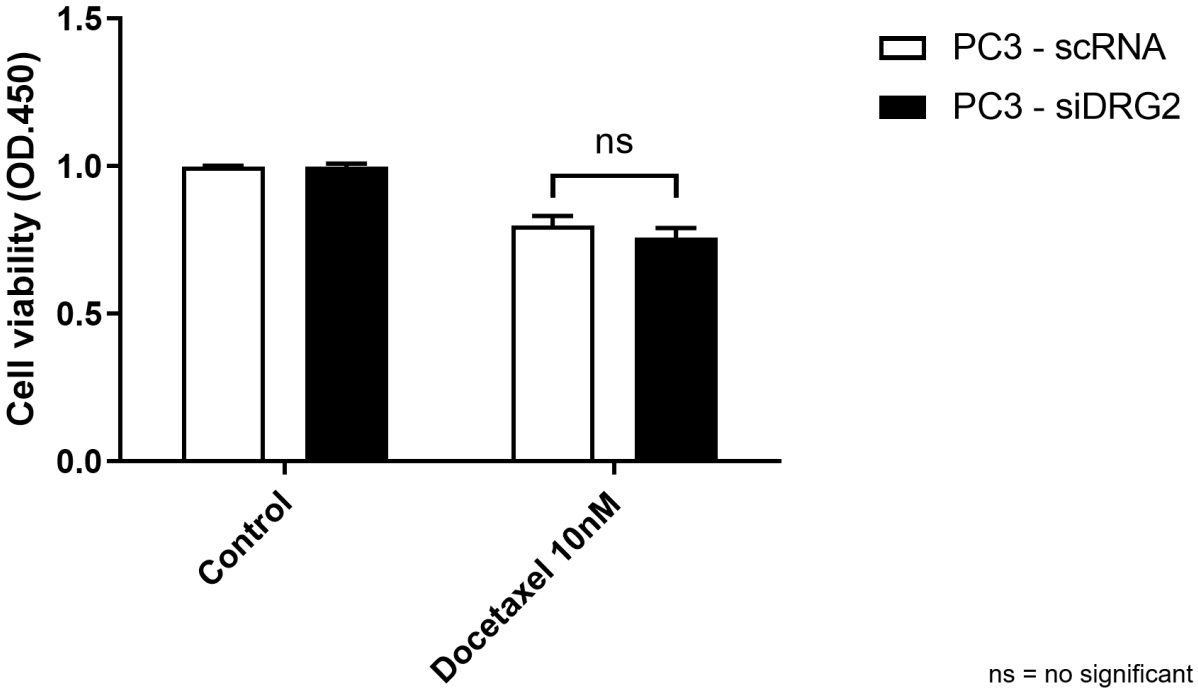

Figure 3h Flow cytometry analysis showing the difference in cell cycles of PC3 transfected with scRNA or siDRG2 after treatment with docetaxel for 72 h. Cell viability was determined using the CCK assay.

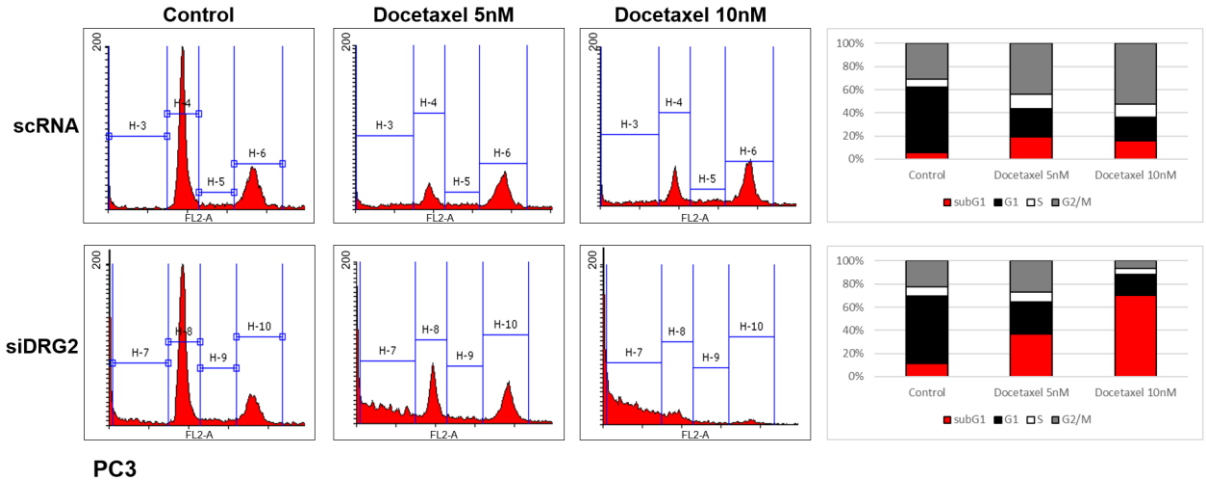

Relationship between PARP inhibitor and DRG2

Differences in the expression of HR-related markers between PC3 and DU145 cells were confirmed using western blotting. We confirmed that the expression of PARP and Rad 51 was high in PC3 cells (Fig. 4a).

When olaparib (10 μM) was added to PC3, which showed an increase in cell number during the recovery period in the previous experiment, no increase in cell number during the recovery period was observed (Fig. 4b).

Cell viability was analyzed after treating PC3 and DU145 cells with docetaxel (5 uM) and olaparib (10 uM) in combination. In PC3 cells, no significant change in cell viability was observed when treated with docetaxel and olaparib alone; however, cell viability significantly decreased after treatment with docetaxel and olaparib in combination. In DU145 cells, no significant change was observed in cell viability after treatment with olaparib alone; however, cell viability significantly decreased after treatment with docetaxel alone and docetaxel and olaparib in combination (Fig. 4c).

Using flow cytometry, the cell cycle phase was evaluated after treating PC3 and DU145 cells with docetaxel (10 nM) and olaparib (10 uM). PC3 cells in the G2/M arrest increased with docetaxel treatment, whereas PC3 cells in the sub-G1 increased with combination treatment. DU145 cells in the sub-G1 increased with both docetaxel alone and combination treatments (Fig. 4d).

Using flow cytometry, changes after treatment with docetaxel (10 nM) and olaparib (10 uM) in PC3 and DU145 cells were evaluated. Annexin V(+)/PI(+) DU145 cells increased with docetaxel treatment, and annexin V(+)/PI(+) DU145 cells increased with docetaxel and olaparib combination treatment; however, this increase was not comparable to the docetaxel treatment. Annexin V(+)/PI(+) PC3 cells increased with docetaxel treatment, and Annexin V(+)/PI(+) PC3 cells increased with docetaxel and olaparib combination treatment (Fig. 4e).

Cell viability of PC3 with p53 null type cells was evaluated after treatment with 15 uM of APR-246, a p53 activator, and docetaxel (10 nM) and olaparib (10 uM) in combination. In PC3 cells not treated

with APR-246, no significant change was observed with docetaxel treatment; however, in PC3 cells treated with APR-246, cell viability was reduced with docetaxel treatment. When APR-246-treated PC3 cells were treated with docetaxel and olaparib in combination, a decrease in cell viability was observed. A similar decrease in cell viability was observed when APR-246-treated PC3 cells were treated with docetaxel alone (Fig. 4f).

Cell viability in DU145 cells after knockdown of p53 was evaluated for combined docetaxel (10 nM) and olaparib (10 uM) treatment. In DU145 cells, cell viability decreased with combined treatment. In sip53 DU145 cells, a significant difference in cell viability was not observed compared to the control (Fig. 4g).

After DRG2 knockdown in PC3 cells, cell viability was evaluated for treatment with docetaxel (10 nM) and olaparib (10 uM). In scRNA PC3 cells, cell viability was confirmed to be reduced with combination treatment compared to docetaxel treatment alone. In siDRG2 PC3 cells, a slight difference in cell viability was observed between docetaxel alone and combination treatments (Fig. 4h).

After overexpression of DRG2 in DU145, cell viability was evaluated after treatment with docetaxel (10 nM) and olaparib (10 uM). In DU145-pcDNA6-V5 cells, cell viability decreased with both docetaxel and combination treatments. However, in DU145-DRG2/pcDNA6-V5 cells, cell viability was significantly reduced with combination treatment compared to docetaxel treatment alone (Fig. 4i).

Figure 4a PARP and Rad 51 expressions in PC3 and DU145 cells as determined via western blot analysis.

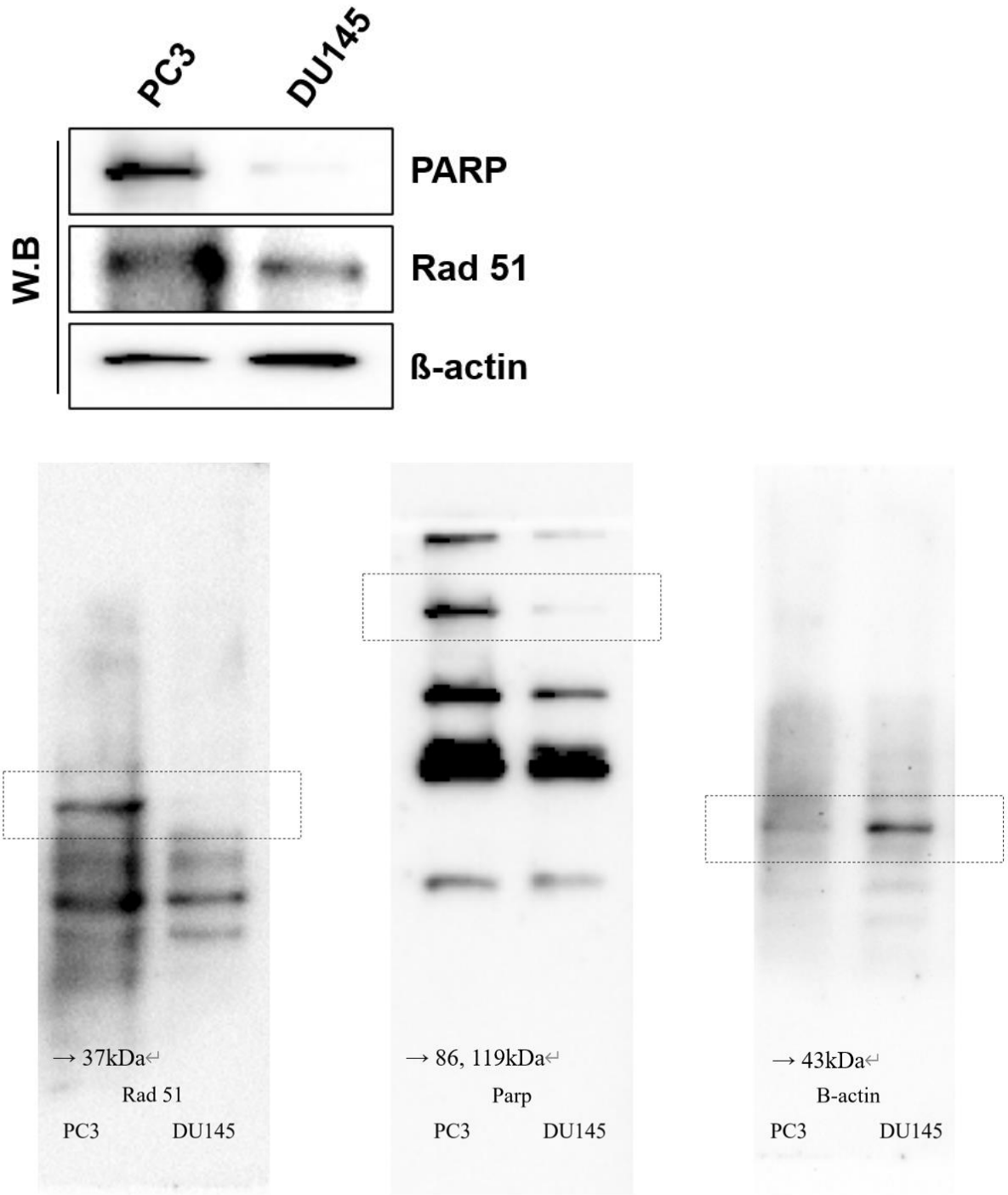

Figure 4b Viability of PC3 cells after treatment with docetaxel and olaparib for 72 h.

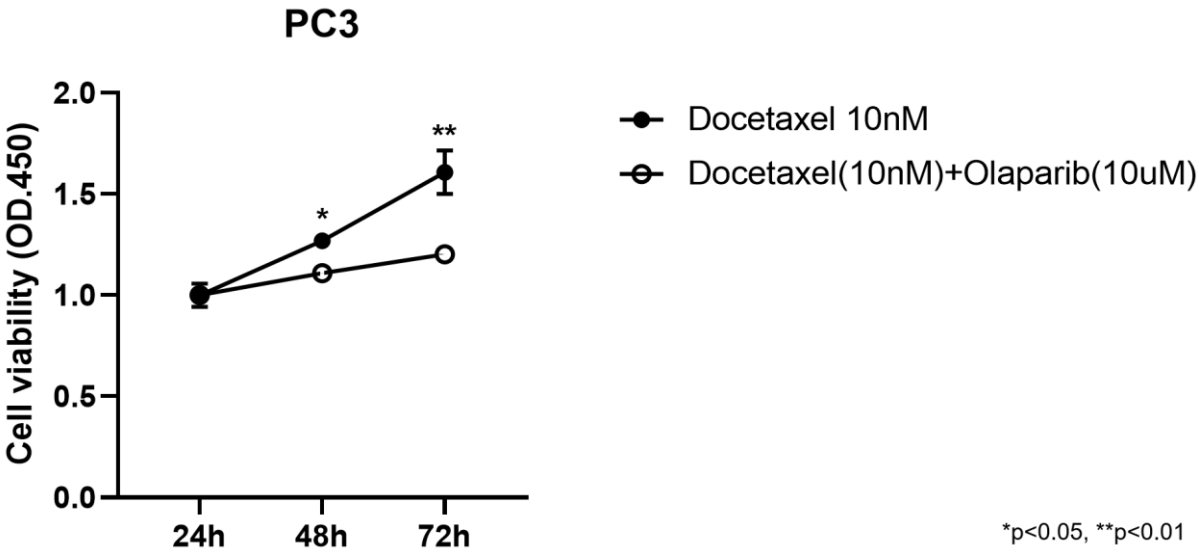

Figure 4c Viability of PC3 and DU145 cells after treatment with docetaxel and olaparib for 72 h.

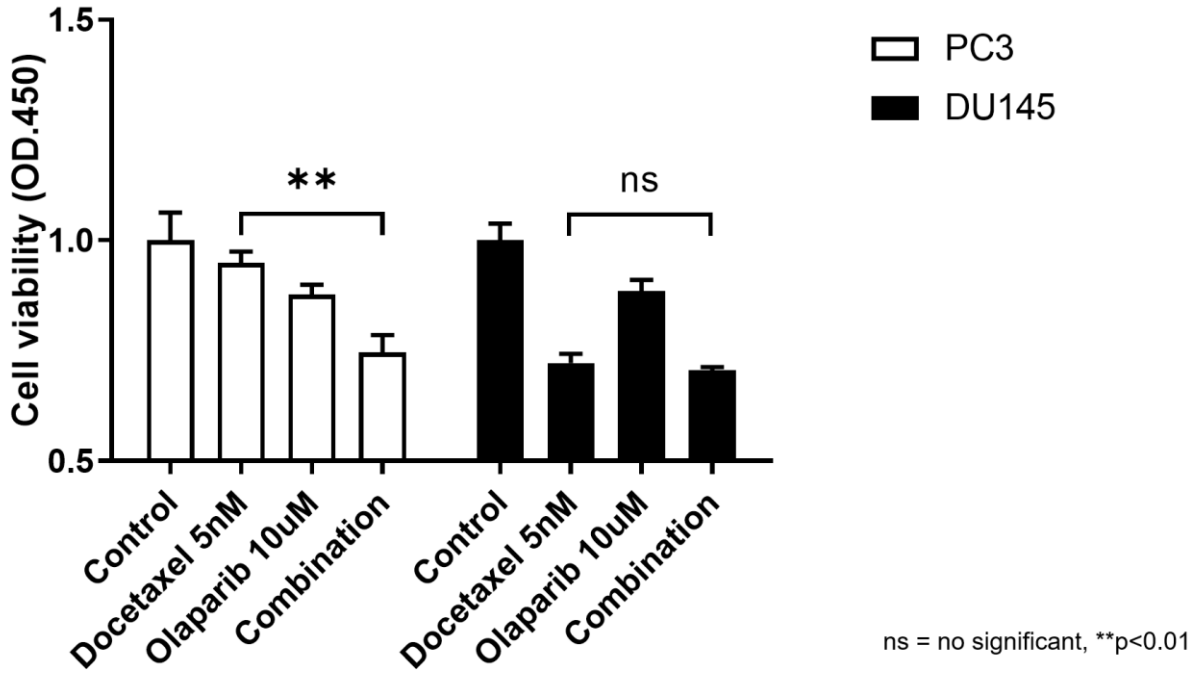

Figure 4d Flow cytometry analysis showing differences in the cell cycle of PC3 and DU145 cells after treatment with docetaxel and olaparib for 72 h.

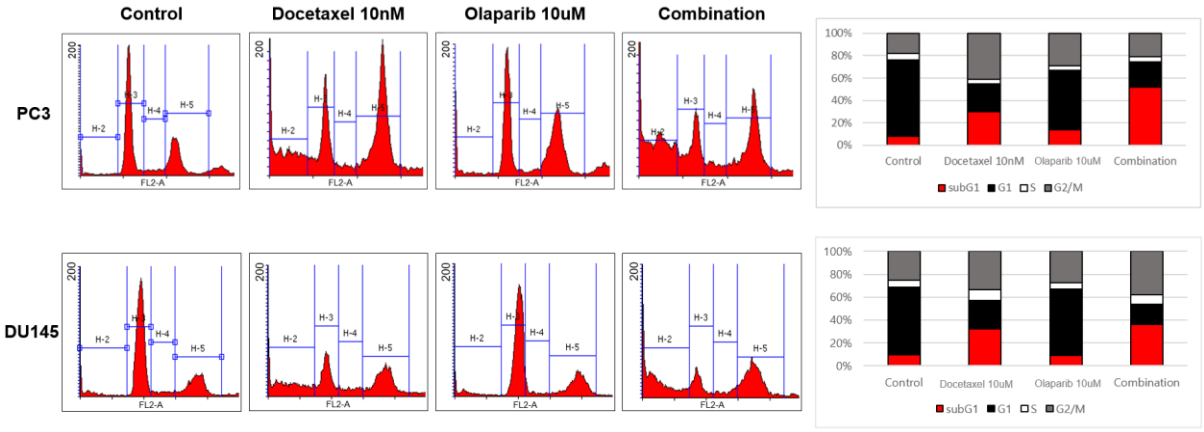

Figure 4e Flow cytometric analysis of PC3 and DU145 cells after treatment with docetaxel and olaparib for 72 h. Cells were stained with Annexin V fluorescein and propidium iodide.

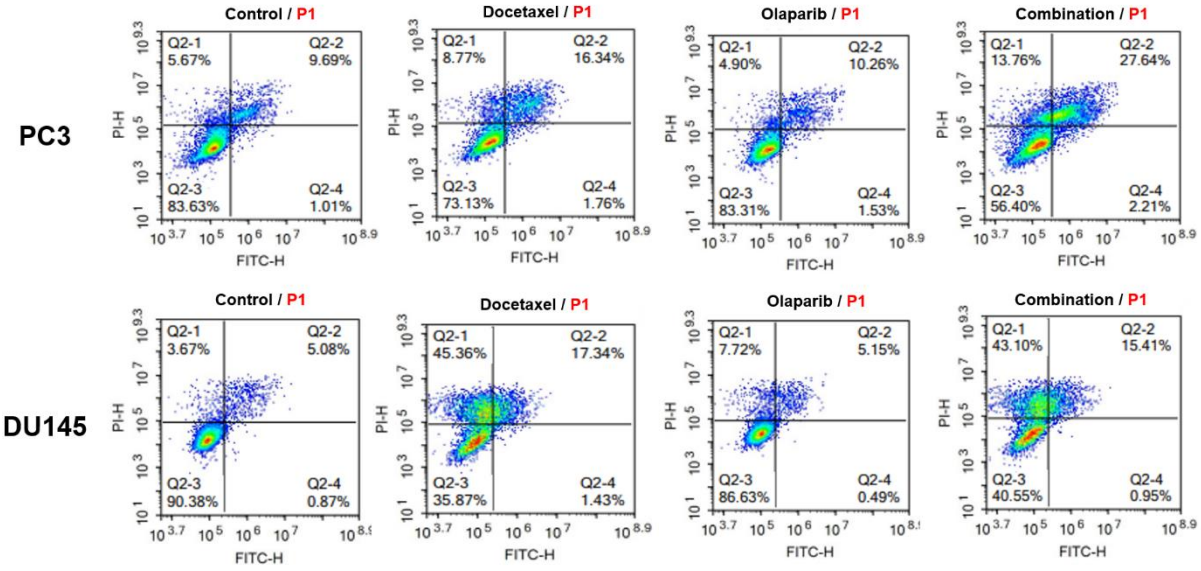

Figure 4f Viability assay of PC3 cells after treatment with APR-246, docetaxel, and olaparib for 72 h.

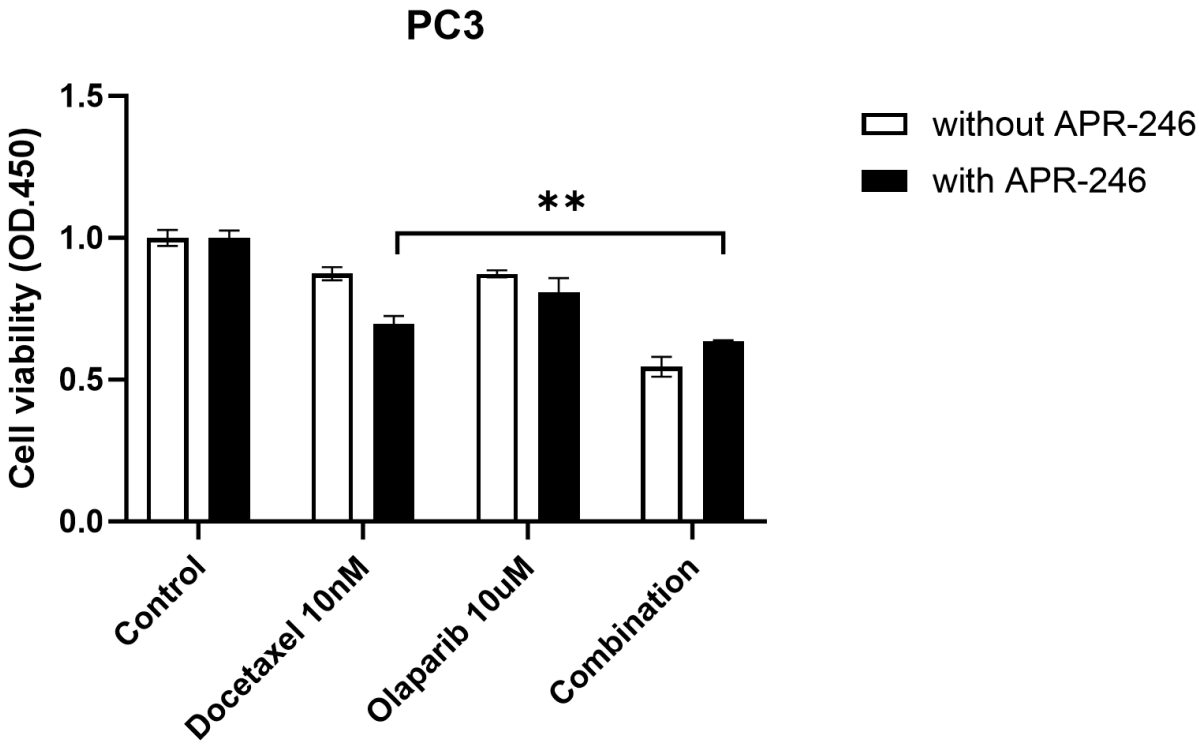

Figure 4g Viability of DU145 cells transfected with scRNA or sip53 after treatment with docetaxel and olaparib for 72 h.

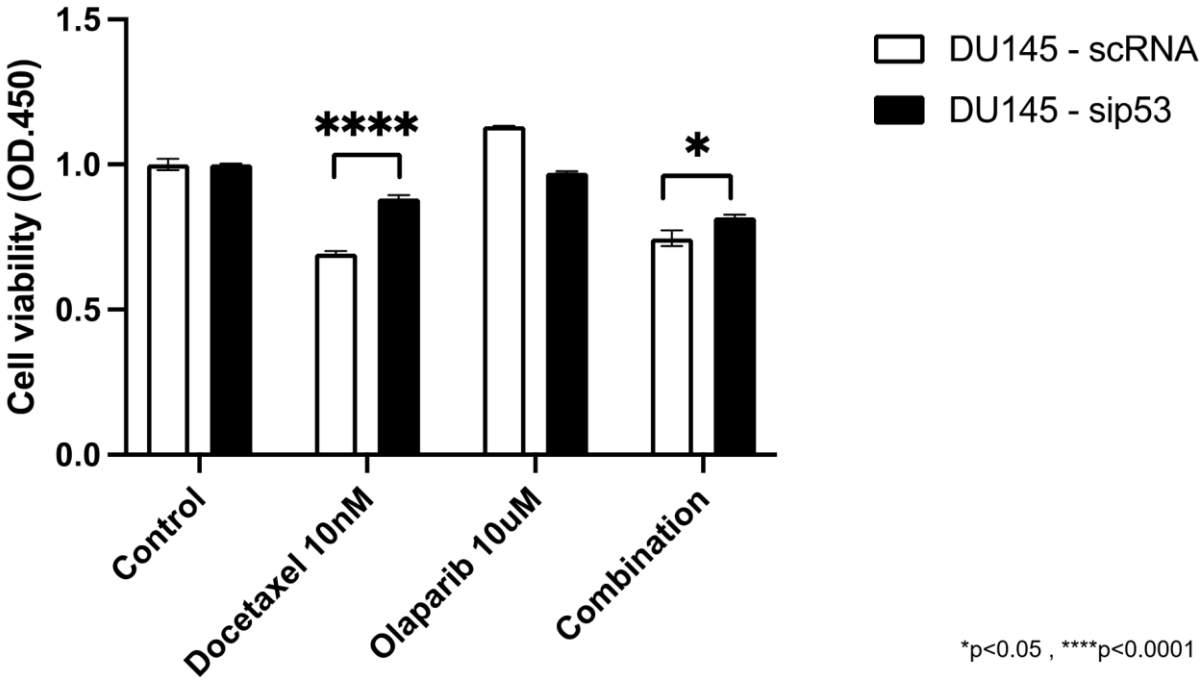

Figure 4h Viability of PC3 cells transfected with scRNA or siDRG2 after treatment with docetaxel and olaparib for 72 h.

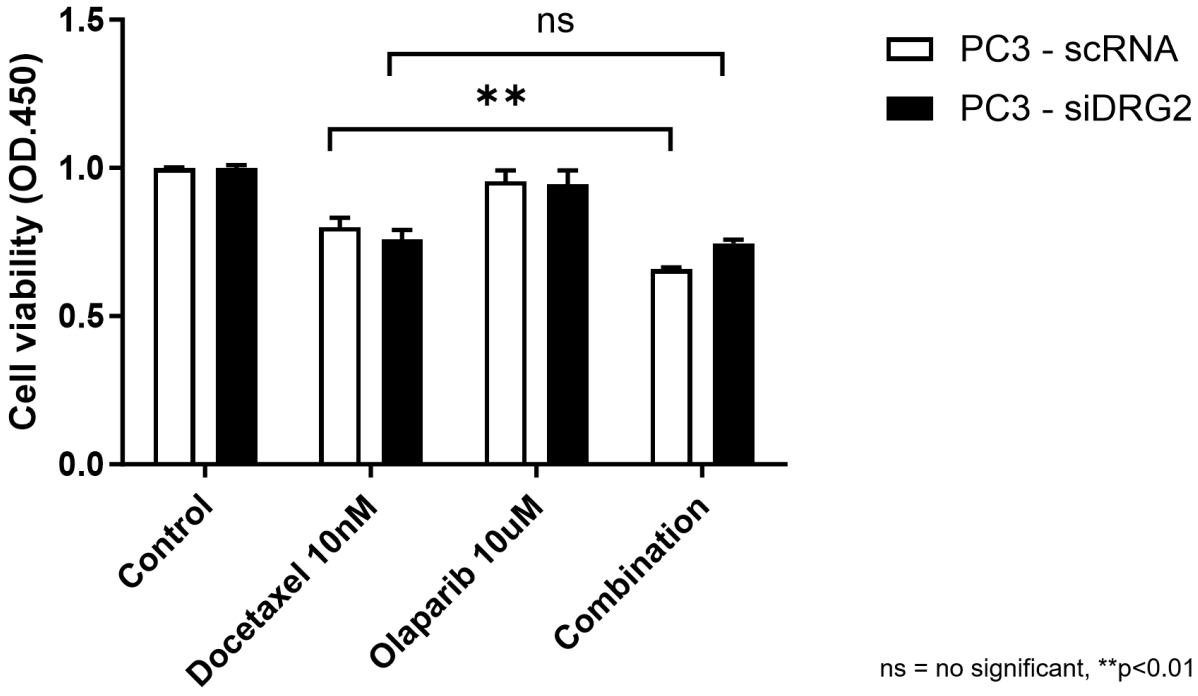

Figure 4i Viability of DU145-pcDNA6-V5 and DU145-DRG2/pcDNA6-V5 cells treated with docetaxel and olaparib for 72 h. Cell viability was determined using the CCK assay.

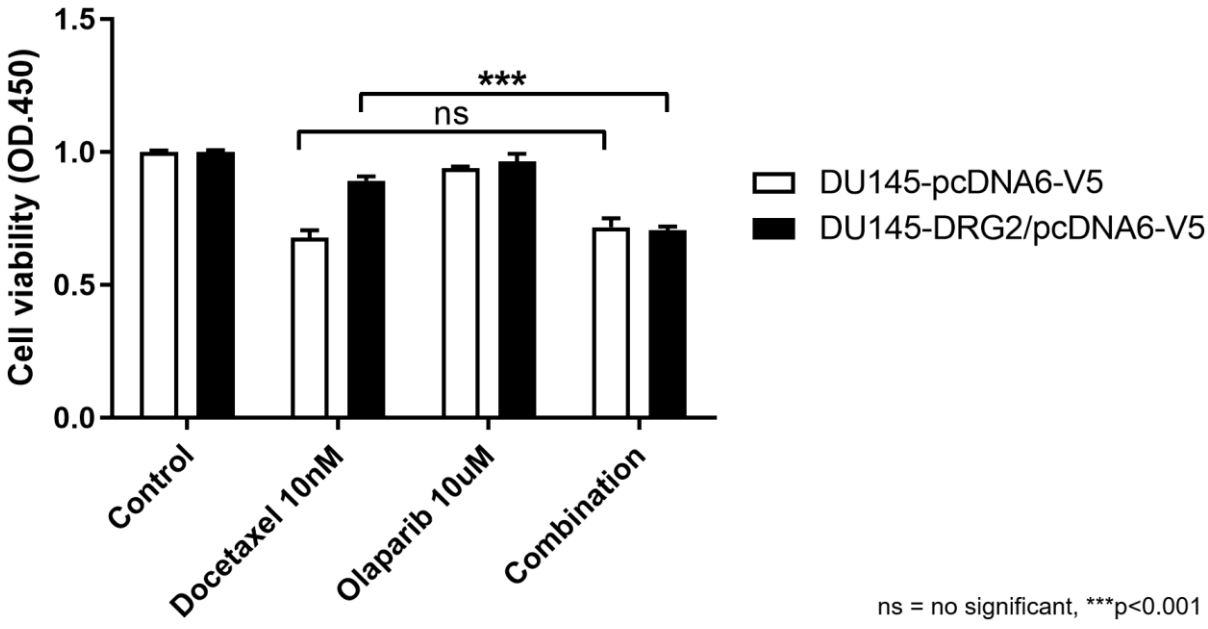

DISCUSSION

Docetaxel-induced cell death in prostate cancer cells may occur with or without the formation of giant cells. In the present study, cell death in PC3 cells occurred with the formation of giant cells. However, cell death in DU145 cells occurred with almost no giant cell formation. Notably, cell death with and without giant cell formation has been termed mitotic catastrophe and apoptosis, respectively [8]. The formation of giant cells is caused by the formation of large cells with multiple micronuclei that appear through mitotic failure [9]. Although many researchers often confuse these two cases during cell death occurs, these two differ fundamentally and occur in different phases of the cell cycle. Lock et al. overexpressed Bcl-2 to prevent apoptosis while treating HeLa cells with etoposide and demonstrated increased catastrophic mitosis [10]. Notably, apoptosis is reported to occur at the G1 checkpoint, whereas mitotic catastrophe occurs mainly at the G2 checkpoint [11].

p53 is the mediator of apoptosis at the G1 checkpoint [12]. Further, p53 controls both the G2/M and the G1 cell cycle checkpoints and mediates reversible growth arrest in human fibroblasts [13]. Therefore, when a cell detects DNA damage, apoptosis occurs at the G1 checkpoint in cells expressing p53, but cells lacking p53 do not undergo G1 arrest and pass over. In the present study, apoptosis in DU145 cells with high p53 expression was confirmed with docetaxel treatment. To verify whether p53 was the cause of these results, the expression of p53 was reversed in PC3 and DU145 cells, and the opposite results were obtained when the cells were treated with docetaxel, indicating that the presence or absence of p53 affects cell viability. Cells that experienced DNA stress but escaped the G1 checkpoint undergo G2/M arrest [14]. In addition, arrest at the G2/M phase increases in cells with higher expression of DRG2 [7] Notably, DRG2 translocates to the nucleus in case of DNA damage. Therefore, DRG2 may mediate cell arrest under DNA stress conditions. In our experiments, G2/M arrest increased when docetaxel was administered to PC3 and LNCaP-LN3 cells with high DRG2 expression levels. G2/M arrest occurred in DU145 cells, in which DRG2 expression was increased with docetaxel treatment by reversing its expression, indicating that DRG2 plays an important role in G2/M cell arrest.

Non-homologous end joining (NHEJ), during DNA repair, acts in the order of G1, S, and G2/M [15]. In contrast, HR has a slight effect on the G1 phase, acts most actively in the S phase, and decreases in the G2/M phase [15]. Notably, NHEJ is more crucial to DNA repair during G2/M than HR [15]. NHEJ will therefore function more if G2/M arrest is prolonged.

PARP expression was observed to be high in PC3 cells but low in DU145 cells via western blotting. PARP plays a role in activating NHEJ [16,17]. Notably, NHEJ is suppressed in PC3 cells, whereas it is active in DU145 cells. NHEJ in PC3 cells is activated upon G2/M arrest. Therefore, PARP plays the main role, and PARP inhibitors play a role in suppressing this [18].

DRG2 plays an important role in G2/M arrest [7]. Therefore, it was expected that G2/M arrest would increase when DNA damage was induced in cells with high DRG2 expression. Notably, in PC3 cells with high DRG2 expression, G2/M arrest increased after docetaxel treatment; however, in DU145 cells with low DRG2 expression, G2/M arrest did not occur. Similar results were obtained when DRG2 was reversed. As cells with high expression of DRG2 were expected to show increased G2/M arrest in our study, indicating a good effect of the PARP inhibitor, increased G2/M arrest in cells expressing DRG2 after docetaxel treatment was expected compared to the PC3 and DU145 cells. However, G2/M arrest increased when PC3 cells with high expression of DRG2 were treated with docetaxel, and cell death occurred with PARP inhibitor treatment. Notably, the same results were obtained when the expression of DRG2 in PC3 and DU145 was reversed under the same conditions.

The present study has some limitations. To determine the effect of the PARP inhibitor, BRCA must be confirmed, but we could not confirm this. In previous studies, PARP inhibitors have been reported to be effective in the BRCA 1/2 mutation [19]. However, in our study, the same results were obtained when DRG2 was reversed in cells, regardless of BRCA. Therefore, the effect of PARP inhibitor appears to be due to DRG2 expression, regardless of BRCA expression. Since docetaxel is an antimicrotubular agent and DRG2 is involved in microtubule formation, docetaxel may be effective against DRG2 due to microtubule activity. However, similar results were obtained with etoposide treatment, which is not an antimicrotubular agent, indicating that microtubule activity is not involved

(Fig. 5). Therefore, understanding the relationship between DRG2 and PARP inhibitors is crucial.

Figure 5a Cell Viability of PC3 and DU145 cells after treatment with etoposide and olaparib for 72 h.

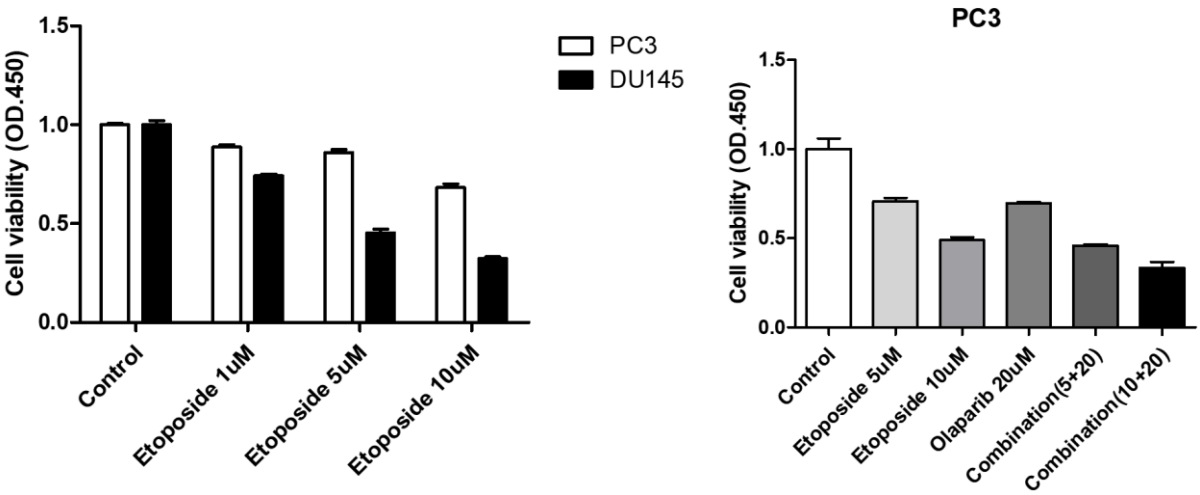

Figure 5b Flow cytometry analysis showing differences in the cell cycle of PC3 and DU145 cells after treatment with etoposide and olaparib for 72 h.

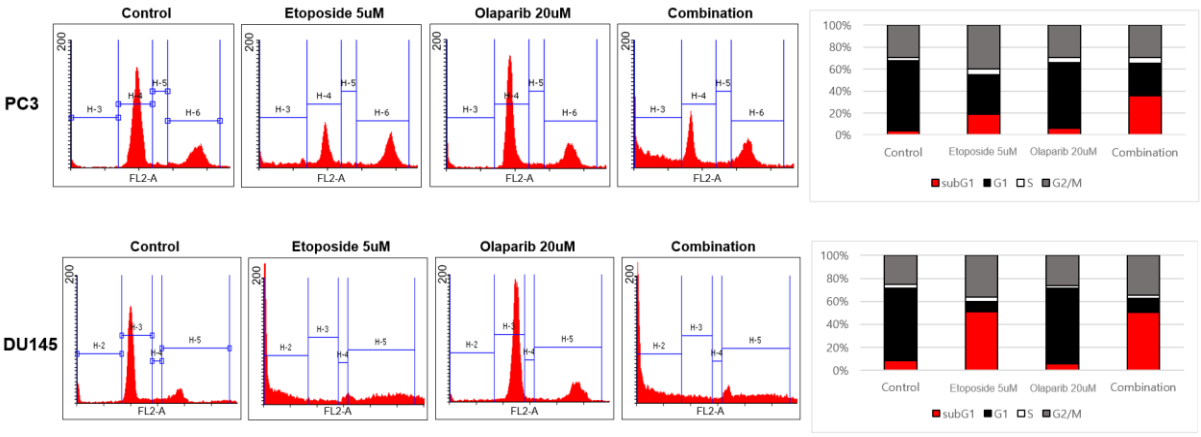

CONCLUSION

DRG2 and p53 expressions play an important role in eliciting the response to docetaxel treatment. In prostate cancer cell lines treated with docetaxel, p53 expression affects apoptosis at the G1 checkpoint, whereas DRG2 expression affects G2/M arrest at the G2 checkpoint. G2/M arrest occurring in DRG2-expressing prostate cancer cell lines in turn affects the response to PARP inhibitors. Therefore, DRG2 expression levels in prostate cancer cell lines can predict the response to PARP inhibitors.

REFERRENCES

1 Siegel, R. L., Miller, K. D., Wagle, N. S. & Jemal, A. Cancer statistics, 2023. *CA Cancer J Clin* **73**, 17-48 (2023). https://doi.org/10.3322/caac.21763

2 Han, H. H. *et al.* Epidemiology of prostate cancer in South Korea. *Prostate Int* **3**, 99-102 (2015). https://doi.org/10.1016/j.prnil.2015.06.003

3 Engels, F. K., Sparreboom, A., Mathot, R. A. & Verweij, J. Potential for improvement of docetaxel-based chemotherapy: a pharmacological review. *Br J Cancer* **93**, 173-177 (2005). https://doi.org/10.1038/sj.bjc.6602698

4 Cai, M. *et al.* Current therapy and drug resistance in metastatic castration-resistant prostate cancer. *Drug Resist Updat* **68**, 100962 (2023). https://doi.org/10.1016/j.drup.2023.100962

5 Clarke, N. W. *et al.* Addition of docetaxel to hormonal therapy in low- and high-burden metastatic hormone sensitive prostate cancer: long-term survival results from the STAMPEDE trial. *Ann Oncol* **30**, 1992-2003 (2019). https://doi.org/10.1093/annonc/mdz396

6 Teyssonneau, D. *et al.* Prostate cancer and PARP inhibitors: progress and challenges. *J Hematol Oncol* **14**, 51 (2021). https://doi.org/10.1186/s13045-021-01061-x

7 Kim, S. C. *et al.* Developmentally regulated GTP-binding protein 2 levels in prostate cancer cell lines impact docetaxel-induced apoptosis. *Investig Clin Urol* **62**, 485-495 (2021). https://doi.org/10.4111/icu.20200574

8 Fabbri, F. *et al.* Mitotic catastrophe and apoptosis induced by docetaxel in hormone-refractory prostate cancer cells. *J Cell Physiol* **217**, 494-501 (2008). https://doi.org/10.1002/jcp.21522

9 Roninson, I. B., Broude, E. V. & Chang, B. D. If not apoptosis, then what? Treatment-induced senescence and mitotic catastrophe in tumor cells. *Drug Resist Updat* **4**, 303-313 (2001). https://doi.org/10.1054/drup.2001.0213

10 Lock, R. B. & Stribinskiene, L. Dual modes of death induced by etoposide in human epithelial tumor cells allow Bcl-2 to inhibit apoptosis without affecting clonogenic survival. *Cancer Res* **56**, 4006-4012 (1996).

11 Portugal, J., Mansilla, S. & Bataller, M. Mechanisms of drug-induced mitotic catastrophe in cancer cells. *Curr Pharm Des* **16**, 69-78 (2010). https://doi.org/10.2174/138161210789941801

12 Aubrey, B. J., Kelly, G. L., Janic, A., Herold, M. J. & Strasser, A. How does p53 induce apoptosis and how does this relate to p53-mediated tumour suppression? *Cell Death Differ* **25**, 104-113 (2018). https://doi.org/10.1038/cdd.2017.169

13 Liao, X. Z. *et al.* Cordycepin Reverses Cisplatin Resistance in Non-small Cell Lung Cancer by Activating AMPK and Inhibiting AKT Signaling Pathway. *Front Cell Dev Biol* **8**, 609285 (2020). https://doi.org/10.3389/fcell.2020.609285

14 Bucher, N. & Britten, C. D. G2 checkpoint abrogation and checkpoint kinase-1 targeting in the treatment of cancer. *Br J Cancer* **98**, 523-528 (2008). https://doi.org/10.1038/sj.bjc.6604208

15 Mao, Z., Bozzella, M., Seluanov, A. & Gorbunova, V. DNA repair by nonhomologous end joining and homologous recombination during cell cycle in human cells. *Cell Cycle* **7**, 2902-2906 (2008). https://doi.org/10.4161/cc.7.18.6679

16 De Lorenzo, S. B., Patel, A. G., Hurley, R. M. & Kaufmann, S. H. The Elephant and the Blind Men: Making Sense of PARP Inhibitors in Homologous Recombination Deficient Tumor Cells. *Front Oncol* **3**, 228 (2013). https://doi.org/10.3389/fonc.2013.00228

17 D'Andrea, A. D. Mechanisms of PARP inhibitor sensitivity and resistance. *DNA Repair (Amst)* **71**, 172-176 (2018). https://doi.org/10.1016/j.dnarep.2018.08.021

18 Chakraborty, A. *et al.* Classical non-homologous end-joining pathway utilizes nascent RNA for error-free double-strand break repair of transcribed genes. *Nat Commun* **7**, 13049 (2016). https://doi.org/10.1038/ncomms13049

19 Lee, J. M., Ledermann, J. A. & Kohn, E. C. PARP Inhibitors for BRCA1/2 mutation-associated and BRCA-like malignancies. *Ann Oncol* **25**, 32-40 (2014). https://doi.org/10.1093/annonc/mdt384

국문요약

서론

DRG2는 도세탁셀 치료 중 미세소관 역학과 G2/M기에서의 세포주기 억제를 조절하는 단백질이다. PARP는 도세탁셀 치료로 인한 DNA 손상에 대해 중요한 복구 시스템으로 작용한다. G2/M기에서의 세포주기 억제는 DNA 복구에 중요한 과정이므로 PARP 저해제와 밀접한 관련이 있다. 본 연구에서는 전립선암 세포주를 이용하여 DRG2 발현이 PARP 저해제에 대한 반응에 끼치는 영향을 조사했다.

재료 및 방법

전립선암 세포주는 PC3, DU145, LNCaP-FGC, and LNCaP-LN3를 사용하였다. 세포 생존율은 세포 카운팅 키트 (CCK)를 이용하여 결정하였으며 DRG2 항체가 웨스턴 블롯에 사용되었다. 세포들은 DRG2 siRNA로 형질 주입되었고, pcDNA6/V5-DRG2는 DRG2를 과발현 하는데 사용되었다. 세포 주기는 유세포분석법을 사용하여 분석되었고, 세포자멸사는 Annexin Ⅴ 세포사멸 검사를 사용하여 검출되었다.

결과

DRG2의 발현은 LNCaP-LN3에서 가장 높았고 DU145 세포에서 가장 낮았다. PC3, DU145, 두 LNCaP 세포주의 p53 발현은 각각 null형, 과발현, 야생형이었다. PC3에서 10nM 도세탁셀은 G2/M기의 세포주기 억제를 증가시켰지만 세포자멸사는 관찰되지 않았다. 그러나 올라파닙을 사용한 후속 치료는 세포자멸사를 촉진했다. DU145 및 LNCaP-FGC에서 10nM 도세탁셀은 sub-G1을 증가시켰지만 G2/M기의 세포주기 억제를 증가시키지 않고

세포 자멸사를 유도한 반면 올라파닙은 추가 효과가 없었다. LNCaP-LN3에서 10nM 도세탁셀로 sub-G1 및 G2/M기의 세포주기 억제 증가가 관찰되었다. 10nM 도세탁셀은 세포자멸사를 유도했고, 추가한 10uM 올라파닙은 세포자멸사를 강화했다. DRG2를 감소시킨 PC3에서 도세탁셀과 올라파닙 조합 치료는 모두 세포자멸사에 거의 영향을 미치지 않았다. DRG2 과발현 DU145에서 세포자멸사는 도세탁셀과 올라파닙 조합에 의해 증가했다.

결론

DRG2 및 p53 발현은 도세탁셀로 치료된 전립선암 세포주에서 중요한 역할을 하며, DRG2 수준은 PARP 저해제에 대한 반응을 예측할 수 있다.